



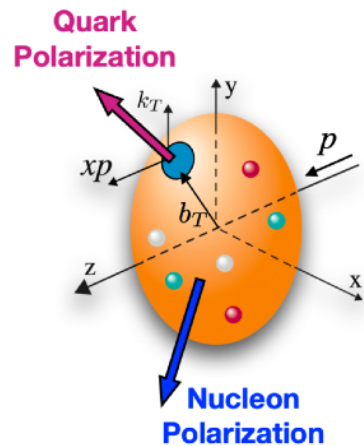
Collins-type Energy-Energy Correlators and Nucleon Structure

Ding-Yu Shao
Fudan University

ECCF2024 Mainz Jul 15 2024

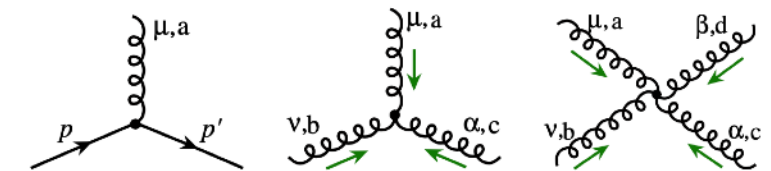
QCD and 3D imaging of nucleon

Transverse momentum distributions (TMDs) encode the quantum correlations between hadron polarization and the motion and polarization of quarks and gluons inside it.



Imaging a hadron would provide insights on QCD

$$-\frac{1}{4}G_{\mu\nu,a}^2[A] + \sum_f \bar{\psi}_f (iD_\mu[A]\gamma^\mu - m_f) \psi_f$$



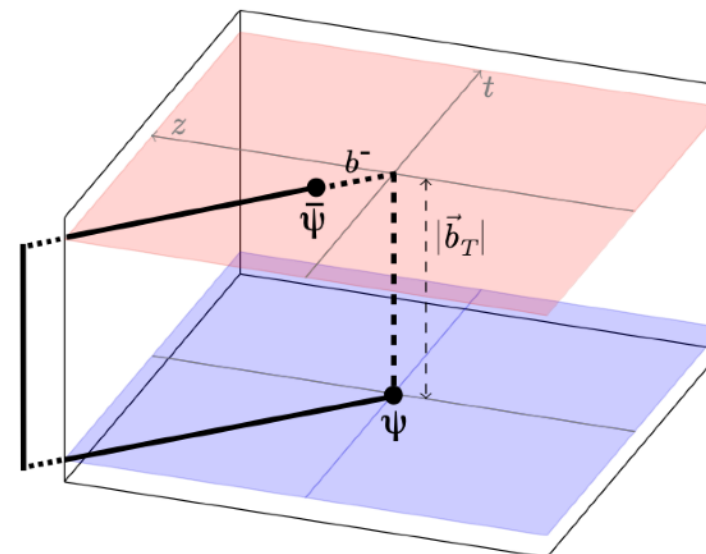
- Both longitudinal and transverse motion

- Large Lorentz boost in longitudinal direction, but not in transverse momentum

- Correlation between hadron **spin** with parton(quark, gluon) **orbital angular momentum**

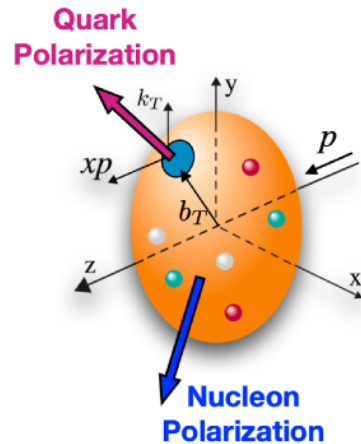
$$\tilde{f}_{i/p_S}^{[\Gamma]0(u)}(x, \mathbf{b}_T, \epsilon, \tau, xP^+) =$$

$$\int \frac{db^-}{2\pi} e^{-ib^-(xP^+)} \left\langle p(P, S) \left| \left[\bar{\psi}^i(b^\mu) W_\square(b^\mu, 0) \frac{\Gamma}{2} \psi^i(0) \right]_\tau \right| p(P, S) \right\rangle$$



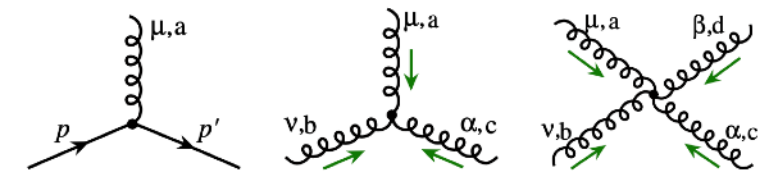
QCD and 3D imaging of nucleon

Transverse momentum distributions (TMDs) encode the quantum correlations between hadron polarization and the motion and polarization of quarks and gluons inside it.



Imaging a hadron would provide insights on QCD

$$-\frac{1}{4}G_{\mu\nu,a}^2[A] + \sum_f \bar{\psi}_f (iD_\mu[A]\gamma^\mu - m_f) \psi_f$$



- Both longitudinal and transverse motion
- Large Lorentz boost in longitudinal direction, but not in transverse momentum
- Correlation between hadron **spin** with parton(quark, gluon) **orbital angular momentum**

$$f_{i/ps}^{[\gamma^+]}(x, \mathbf{k}_T, \mu, \zeta) = f_1(x, k_T) - \frac{\epsilon_T^{\rho\sigma} k_{T\rho} S_{T\sigma}}{M} \kappa f_{1T}^\perp(x, k_T),$$

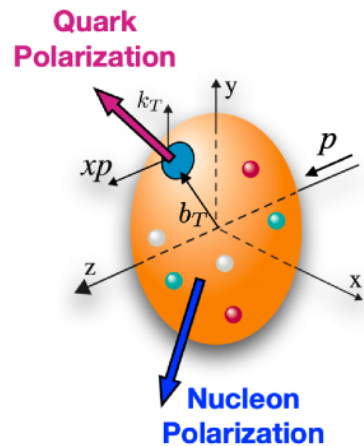
$$f_{i/ps}^{[\gamma^+\gamma^5]}(x, \mathbf{k}_T, \mu, \zeta) = S_L g_1(x, k_T) - \frac{k_T \cdot S_T}{M} g_{1T}^\perp(x, k_T),$$

$$f_{i/ps}^{[i\sigma^{\alpha+}\gamma^5]}(x, \mathbf{k}_T, \mu, \zeta) = S_T^\alpha h_1(x, k_T) + \frac{S_L k_T^\alpha}{M} h_{1L}^\perp(x, k_T)$$

$$- \frac{\mathbf{k}_T^2}{M^2} \left(\frac{1}{2} g_T^{\alpha\rho} + \frac{k_T^\alpha k_T^\rho}{\mathbf{k}_T^2} \right) S_{T\rho} h_{1T}^\perp(x, k_T) - \frac{\epsilon_T^{\alpha\rho} k_{T\rho}}{M} \kappa h_1^\perp(x, k_T)$$

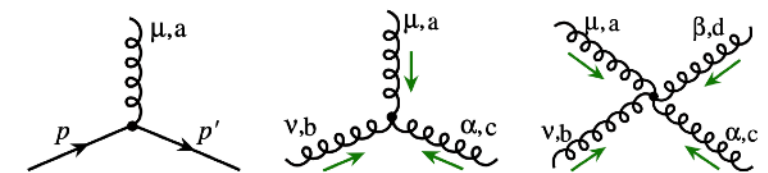
QCD and 3D imaging of nucleon

Transverse momentum distributions (TMDs) encode the quantum correlations between hadron polarization and the motion and polarization of quarks and gluons inside it.



Imaging a hadron would provide insights on QCD

$$-\frac{1}{4}G_{\mu\nu,a}^2[A] + \sum_f \bar{\psi}_f (iD_\mu[A]\gamma^\mu - m_f) \psi_f$$



- Both longitudinal and transverse motion
- Large Lorentz boost in longitudinal direction, but not in transverse momentum
- Correlation between hadron **spin** with parton(quark, gluon) **orbital angular momentum**

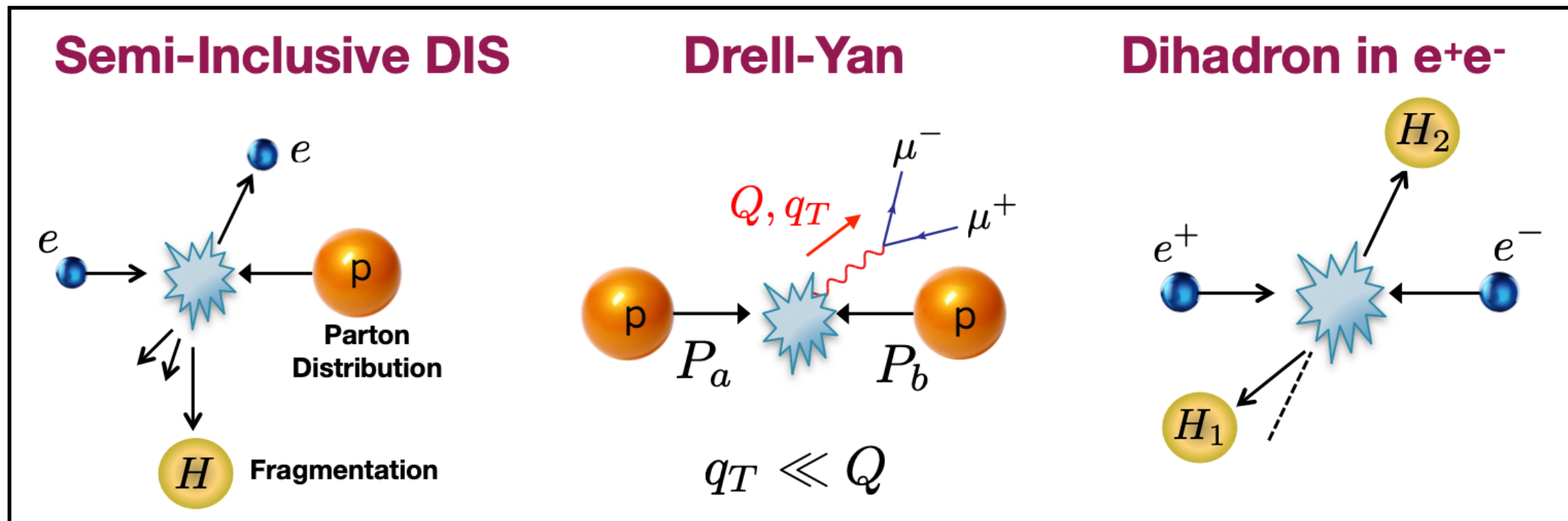
TMDs		Quark Polarization		
		Unpolarized (U)	Longitudinally polarized (L)	Transversely polarized (T)
Nucleon Polarization	U	f_1 unpolarized		h_1^\perp Boer-Mulders
	L		g_{1L} helicity	h_{1L}^\perp longi-transversity
	T	f_{1T}^\perp Sivers	g_{1T} trans-helicity	h_1 transversity h_{1T}^\perp pretzelosity

Nucleon spin
 Quark spin

Figure 2.5: The leading-twist quark TMD distributions.

Transverse momentum distributions of quarks

- Three classical processes used to probe quark TMDs

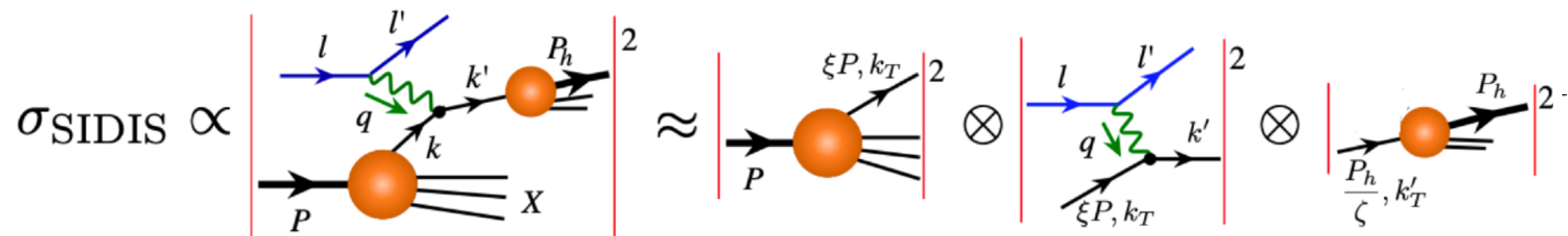
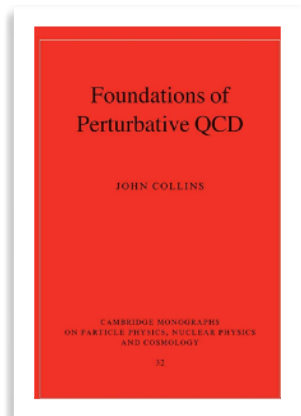


- Typical “two-scale” problem:
transverse momentum of final particle (q_T) \ll scattering energy (Q)
- Theory tools: factorization theorem; renormalization group evolution; effective field theory ...

Theory Formalism in Semi-Inclusive DIS

$$e(\ell) + p(P, \mathbf{S}_\perp) \rightarrow e(\ell') + h(P_h) + X$$

TMD factorization theorems have been established at the leading power of q_T^2/Q^2



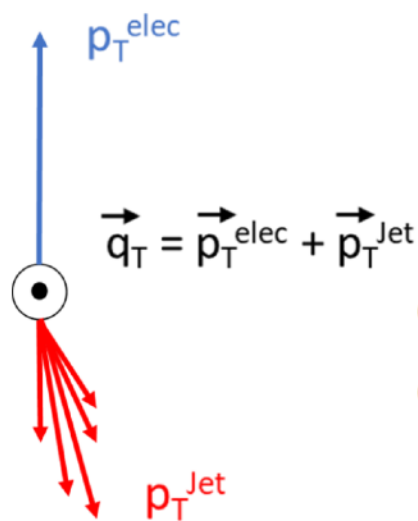
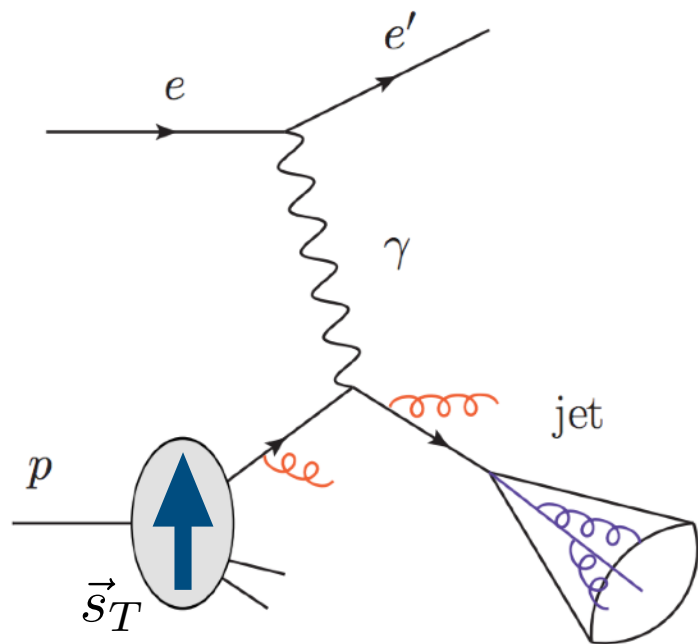
Theory framework: Collins-Soper-Sterman, Ji-Ma-Yuan, Soft-Collinear Effective Theory

$$\frac{d\sigma(ep \rightarrow ehX)}{dQ dx dz d\vec{q}_T} = H_{eq \rightarrow eq}(Q) F_q(\vec{q}_T, x) \otimes D_{q \rightarrow h}(\vec{q}_T, z)$$

Some recent progresses on factorization theorem at the sub-leading power see:

Bacchetta, Boer, Diehl, Mulders '08; Chen, Ma'16, Bacchetta, G. Bozzi, M. G. Echevarria, C. Pisano, A. Prokudin and M. Radici '19; Vladimirov, Moos and Scimemi, '21; Rodini, Vladimirov, '22; Ebert, Gao, Stewart '22; Gamberg, Kang, DYS, Terry, Zhao '22...

QCD jets and 3D proton imaging at the EIC

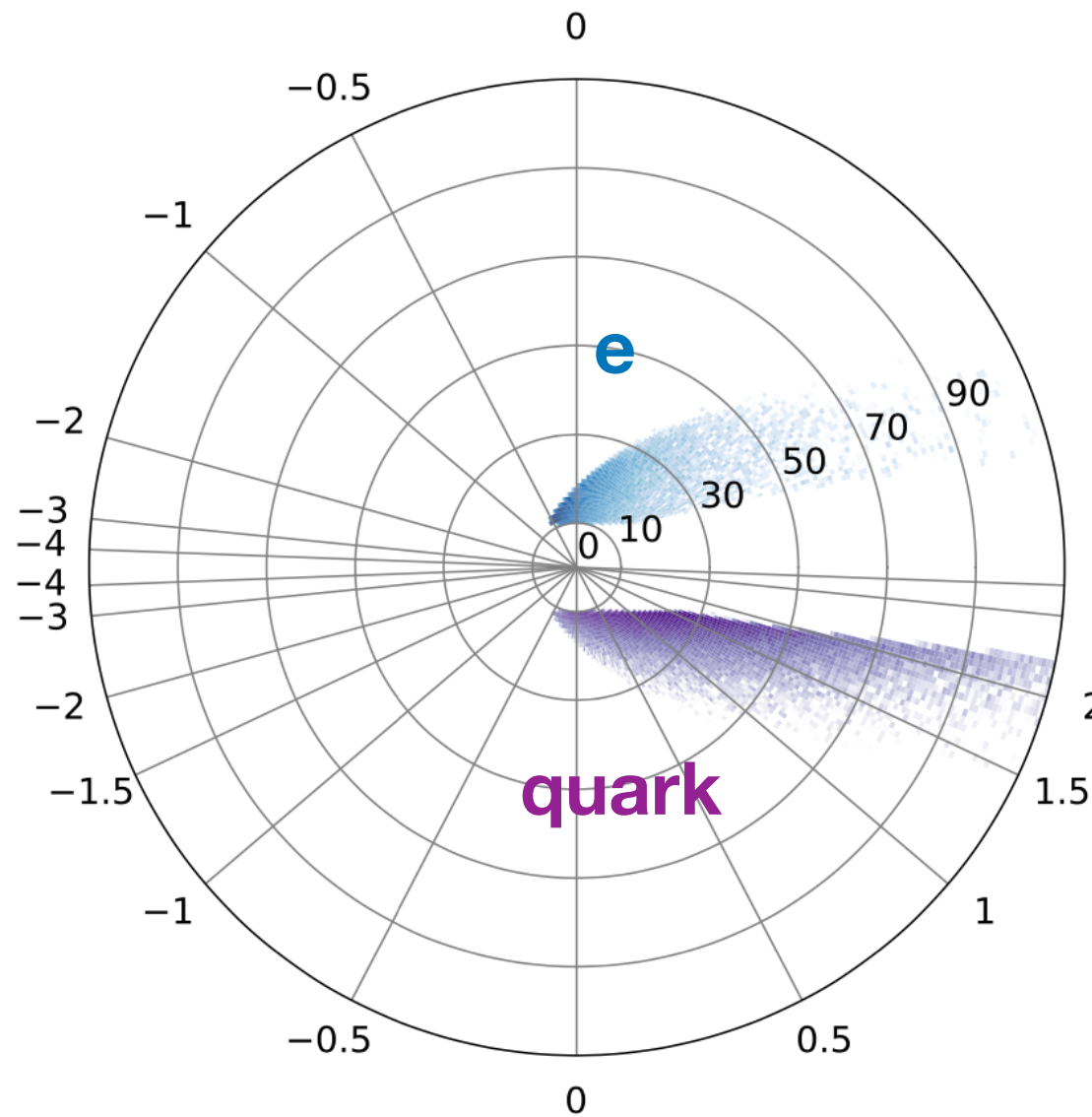


- Recent investigations at both the RHIC and LHC have validated jets as effective tools for probing the spin structure of the nucleon.
- Jets are complementary to standard SIDIS extractions of TMDs
- Jet measurements allow independent constraints on TMD PDFs and FFs from a single measurement
- Azimuthal correlation between jet and lepton sensitive to TMD PDFs (X. Liu, Ringer, Vogelsang, F. Yuan '19 PRL,

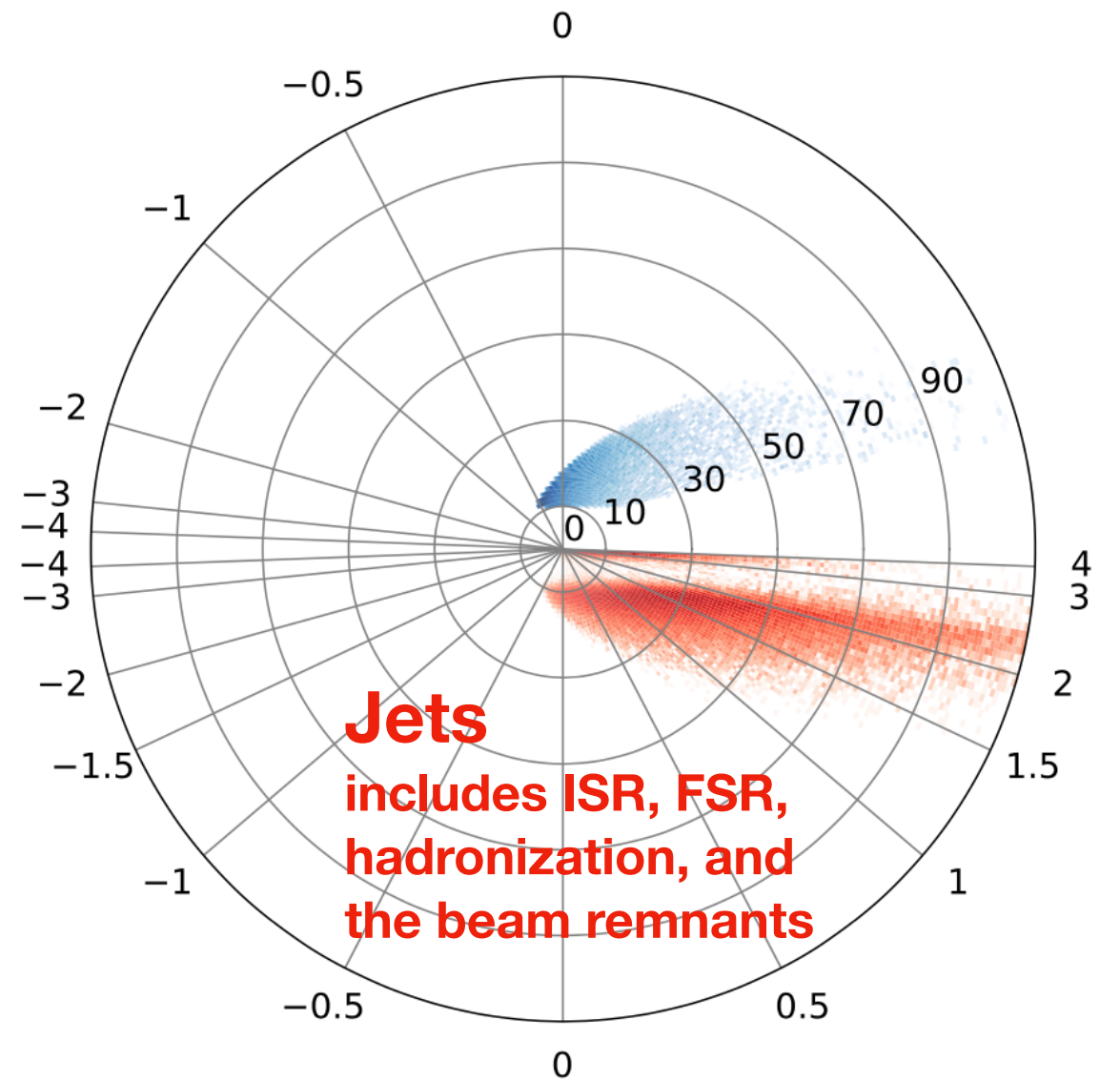
Simulation results

Arratia, Kang, Prokudin, Ringer '19

10 + 275 GeV,
 $0.1 < y < 0.85, p_T^e > 10 \text{ GeV}$

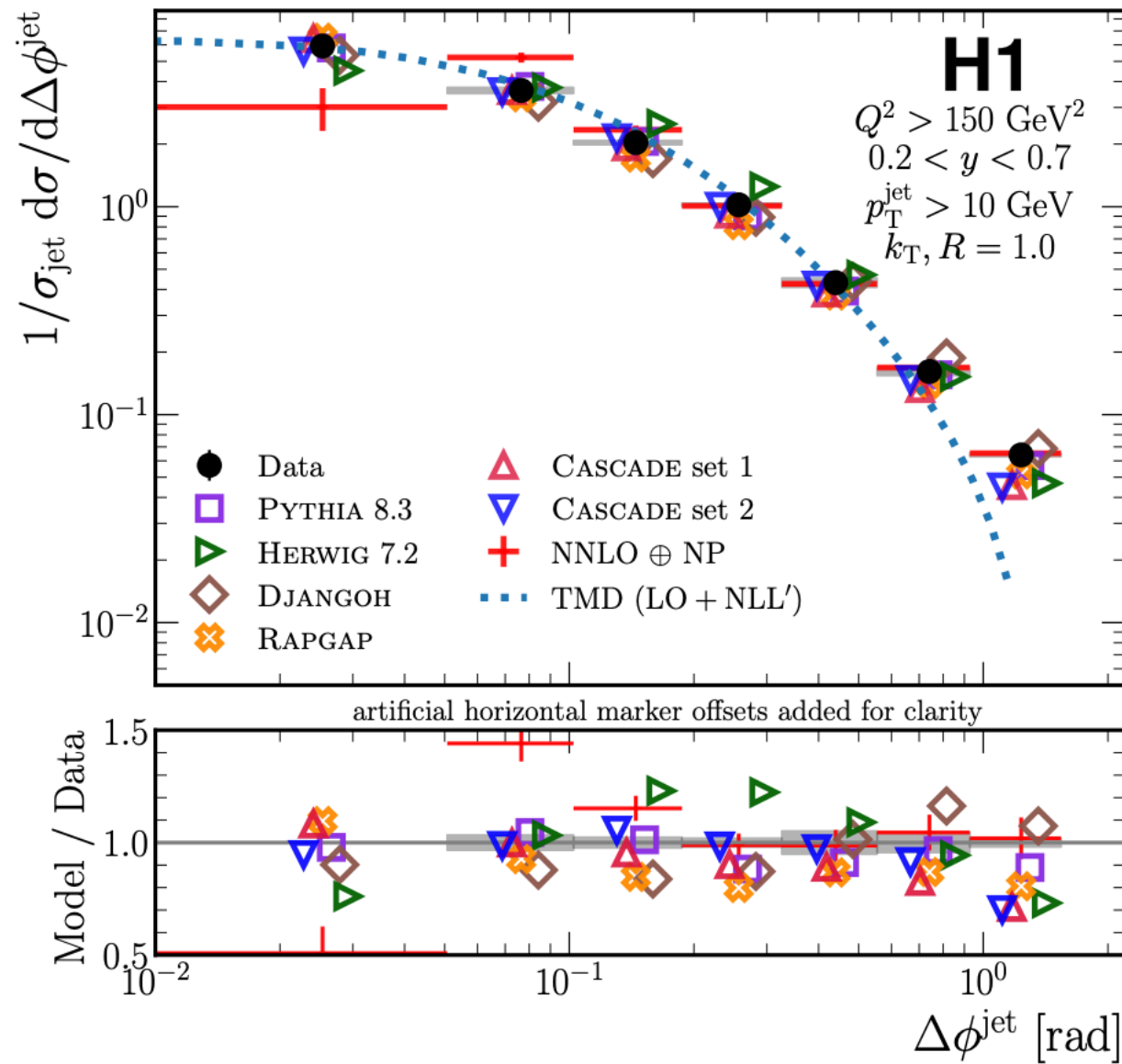


10 + 275 GeV,
 $0.1 < y < 0.85, p_T^e > 10 \text{ GeV}$

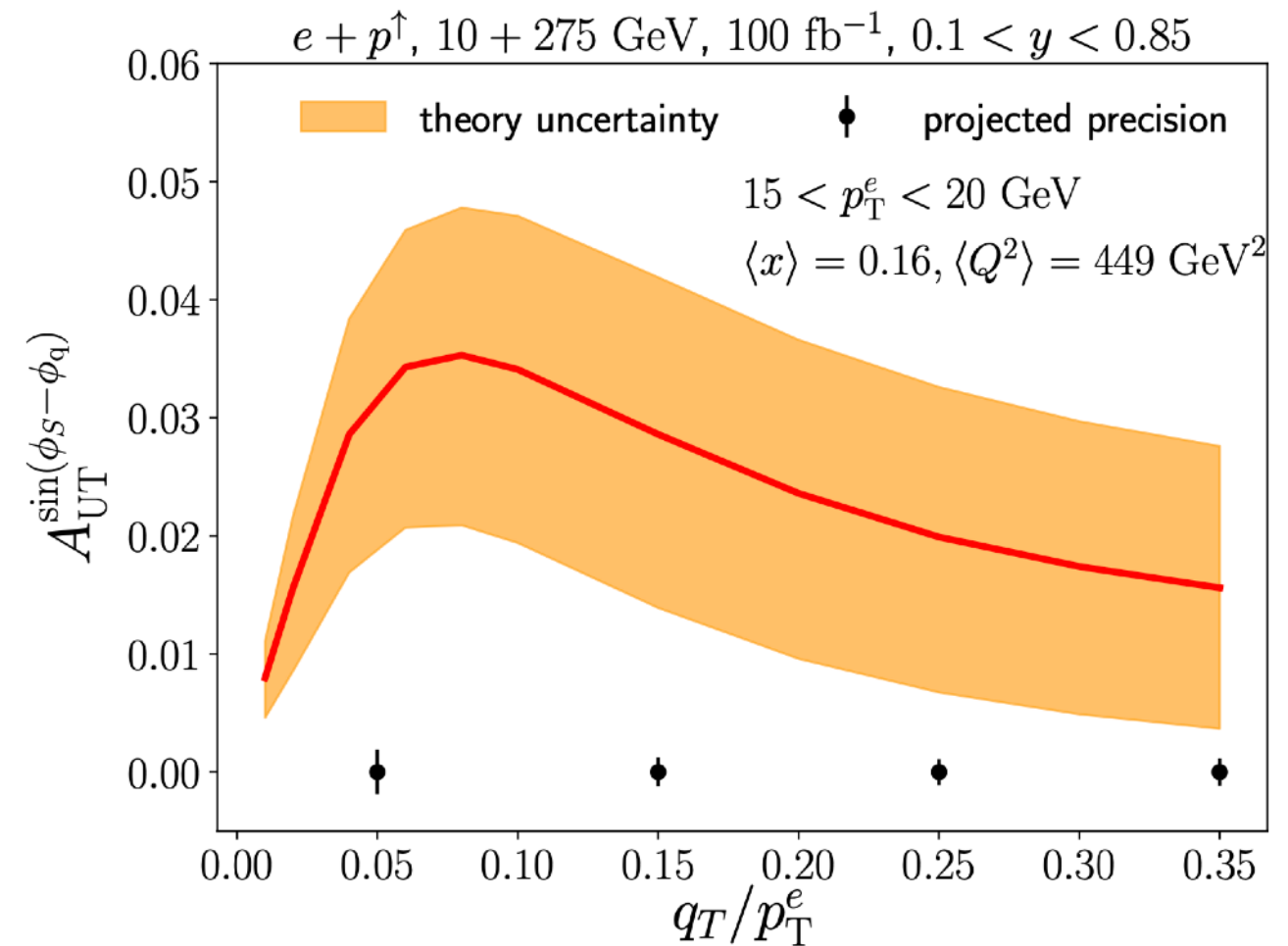


The jet distribution matches the struck-quark kinematics

Theory predictions and measurements in DIS



H1 collaboration, '22



Arratia, Kang, Prokudin, Ringer '19

Recoil-free azimuthal angle for electron-jet correlation

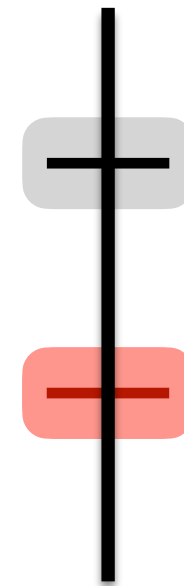
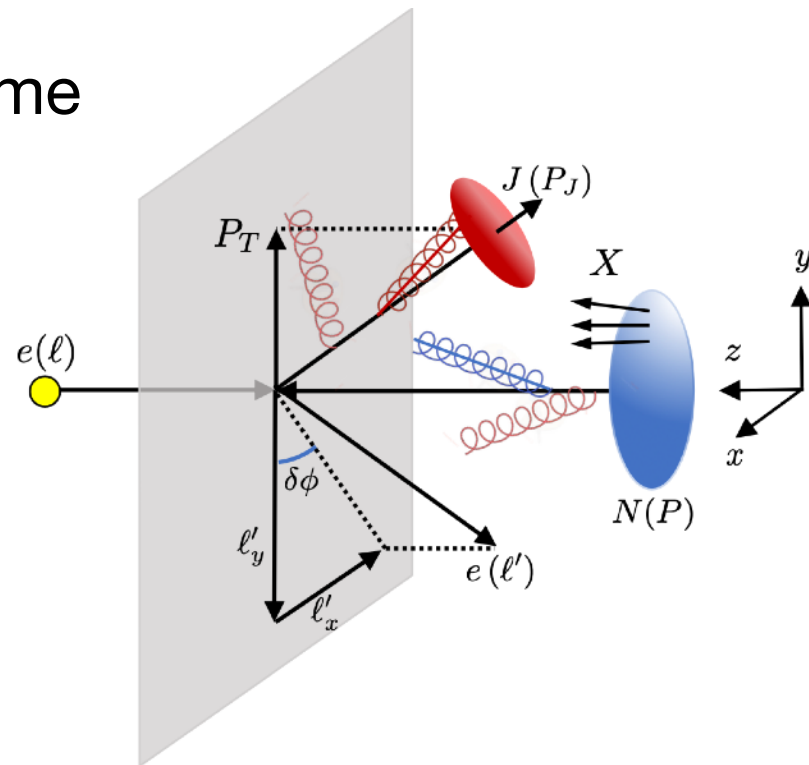
Fang, Ke, DYS, Terry '23 JHEP

$$e(\ell) + N(P) \rightarrow e(\ell') + J(P_J) + X$$

Standard TMD in back to back limit: $Q \gg q_T \sim l_T \delta\phi$

Chien, Rahn, DYS, Waalewijn & Wu '22 JHEP + Schrignder '21 PLB

Lab frame



$$p_h \sim Q(1, 1, 1)$$

$$p_{c_i}^\mu \sim l_T (\delta\phi^2, 1, \delta\phi)_{n_i \bar{n}_i}$$

$$p_s^\mu \sim l_T (\delta\phi, \delta\phi, \delta\phi)$$

Similar to Transverse-EEC in back to back

Following the standard steps in SCET and CSS, we obtain the following resummation formula

$$\frac{d\sigma}{d^2\ell'_T dy d\delta\phi} = \frac{\sigma_0 \ell'_T}{1-y} H(Q, \mu) \int_0^\infty \frac{db}{\pi} \cos(b\ell'_T \delta\phi) \sum_q e_q^2 f_{q/N}(x_B, b, \mu, \zeta_f) J_q(b, \mu, \zeta_J)$$

Hard factor

Fourier transformation
in 1-dim

TMD PDF

Jet function

Predictions in e-p

Fang, Ke, DYS, Terry '23

TMD PDF (CSS treatment)

$$f_{q/N}(x_B, b, \mu, \zeta_f) = [C \otimes f]_{q/N}(x_B, b, \mu_f, \zeta_{fi}) U_{\text{NP}}^f(x_B, b, A, Q_0, \zeta_f) \times \exp \left[\int_{\mu_f}^{\mu} \frac{d\mu'}{\mu'} \gamma_{\mu}^f(\mu', \zeta_f) \right] \left(\frac{\zeta_f}{\zeta_{fi}} \right)^{\frac{1}{2} \gamma_{\zeta}^f(b, \mu_f)},$$

Jet function

$$J_q(b, \mu, \zeta_J) = J_q(b, \mu_J, \zeta_{Ji}) U_{\text{NP}}^J(b, A, Q_0, \zeta_J) \times \exp \left[\int_{\mu_J}^{\mu} \frac{d\mu'}{\mu'} \gamma_{\mu}^J(\mu', \zeta_J) \right] \left(\frac{\zeta_J}{\zeta_{Ji}} \right)^{\frac{1}{2} \gamma_{\zeta}^J(b, \mu_J)}$$

scale choice

$$\mu_H = Q, \quad \mu_f = \mu_J = \sqrt{\zeta_{fi}} = \sqrt{\zeta_{Ji}} = \mu_b = 2e^{-\gamma_E}/b$$

b*-prescription to avoid Landau pole

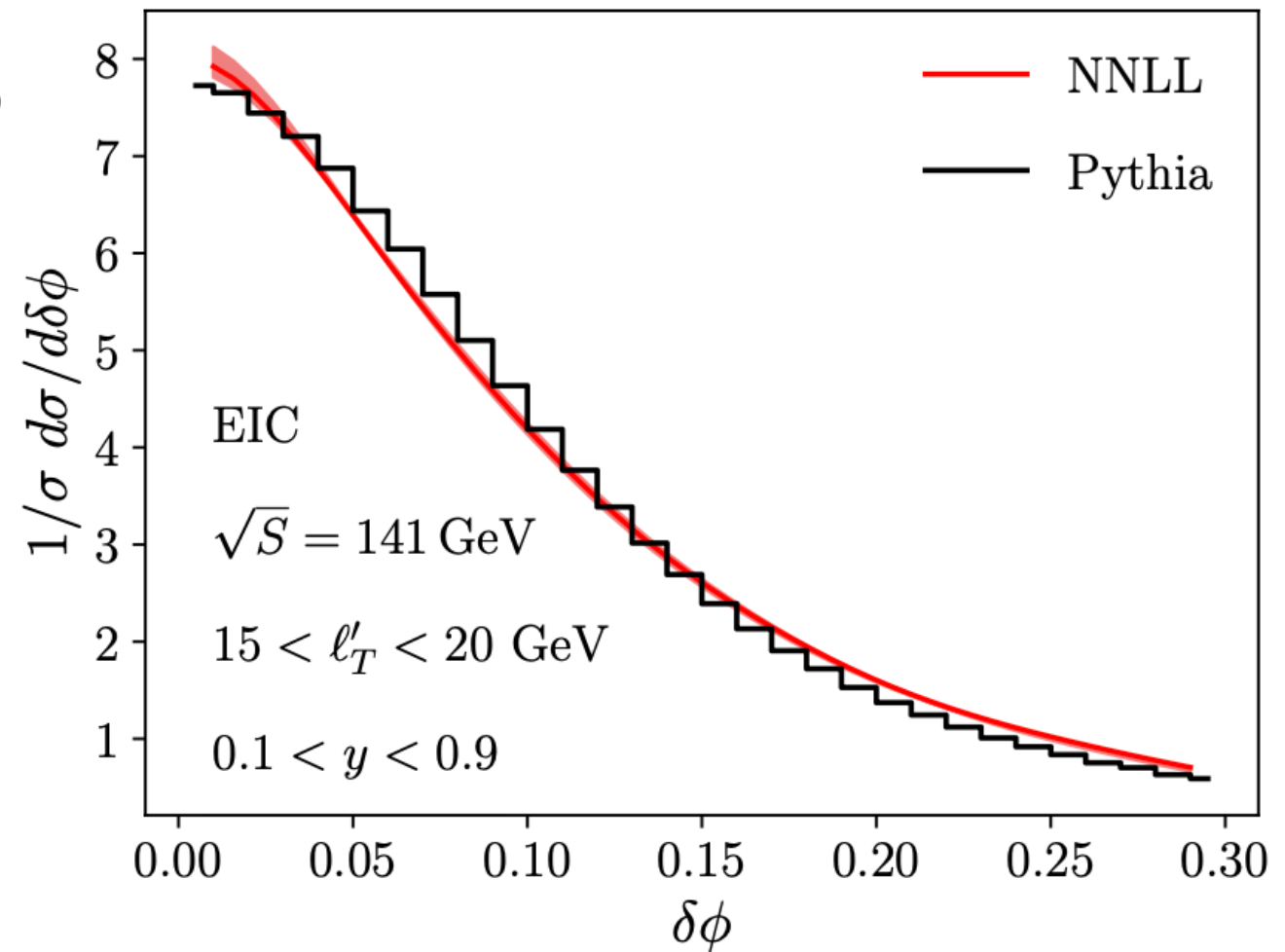
$$b_* = b / \sqrt{1 + b^2/b_{\text{max}}^2} \quad \mu_{b_*} = 2e^{-\gamma_E}/b_*$$

non-perturbative model

$$U_{\text{NP}}^f = \exp \left[-g_1^f b^2 - \frac{g_2}{2} \ln \frac{Q}{Q_0} \ln \frac{b}{b_*} \right]$$

$$U_{\text{NP}}^J = \exp \left[-\frac{g_2}{2} \ln \frac{Q}{Q_0} \ln \frac{b}{b_*} \right]$$

Sun, Isaacson, Yuan, Yuan '14



μ_H varies between $Q/2$ and $2Q$. μ_b is fixed

Predictions in e-A

Fang, Ke, DYS, Terry '23

We apply nuclear modified TMD PDFs

$$g_1^A = g_1^f + a_N(A^{1/3} - 1) \quad a_N = 0.016 \pm 0.003 \text{ GeV}^2$$

Collinear dynamics (nPDF) using EPPS16

(Alrashed, Anderle, Kang, Terry & Xing, '22)

We include LO momentum broadening of the jet within SCET_G

$$J_q^A(b, \mu, \zeta_J) = J_q(b, \mu, \zeta_J) e^{\chi[\xi b K_1(\xi b) - 1]}$$

Opacity parameter $\chi = \frac{\rho_G L}{\xi^2} \alpha_s(\mu_{b_*}) C_F$

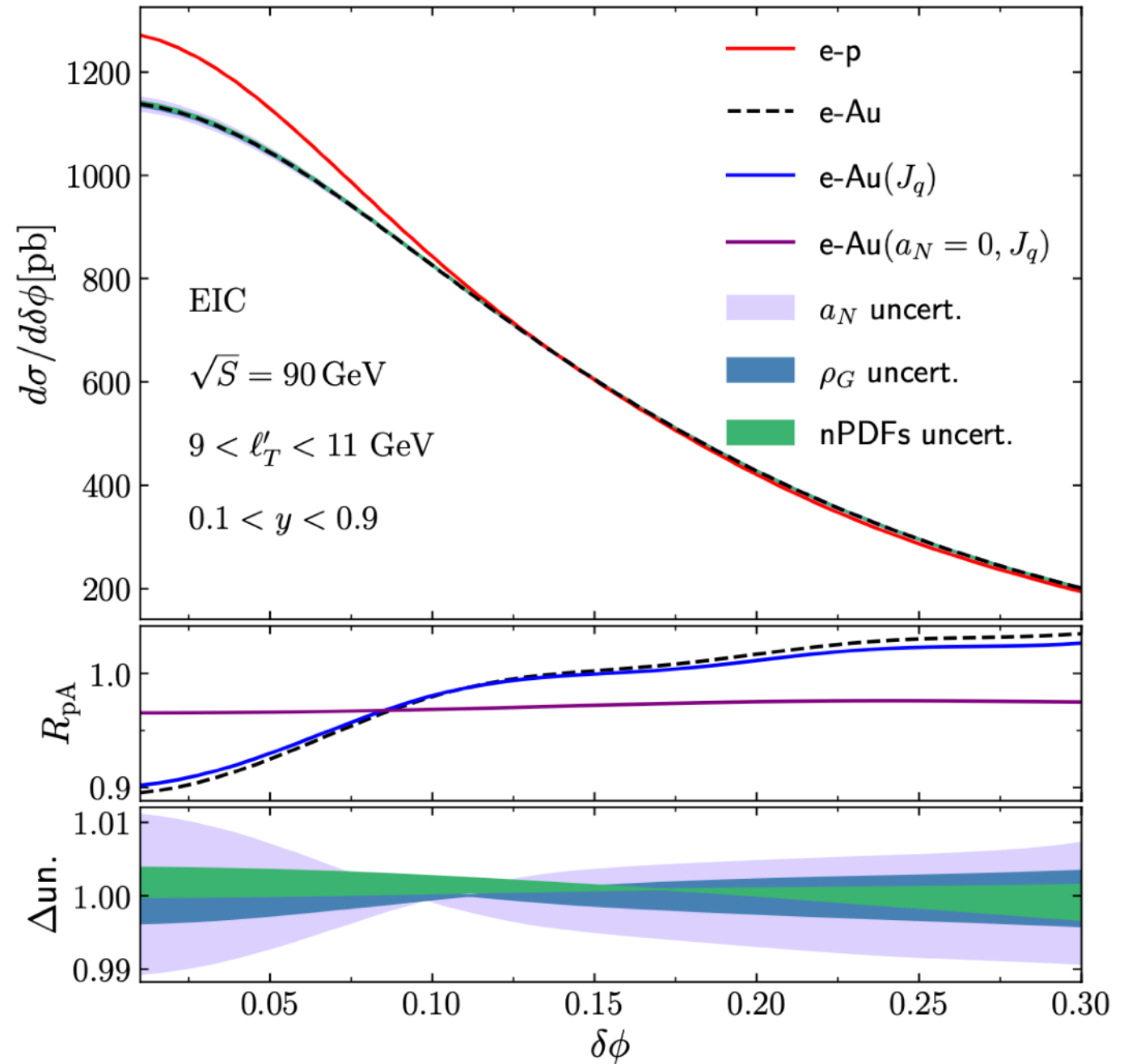
(Gyulassy, Levai, & Vitev '02)

ρ_G : density of the medium

ξ : the screening mass

L: the length of the medium

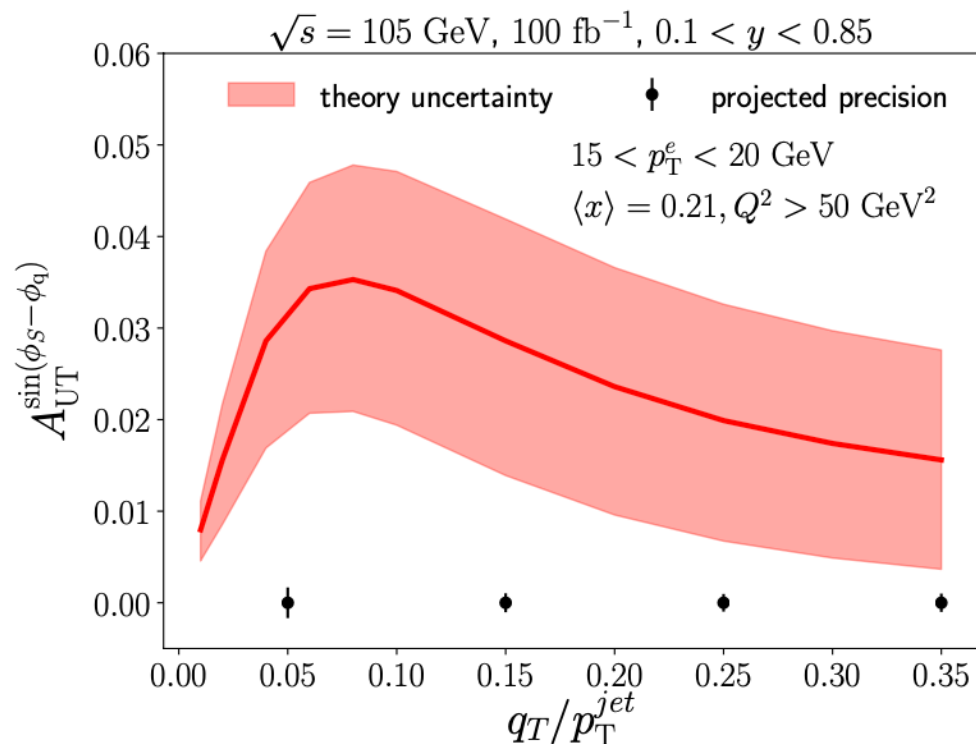
Parameter values are taken from a recent comparison between SCET_G in e-A from the HERMES Ke and Vitev '23



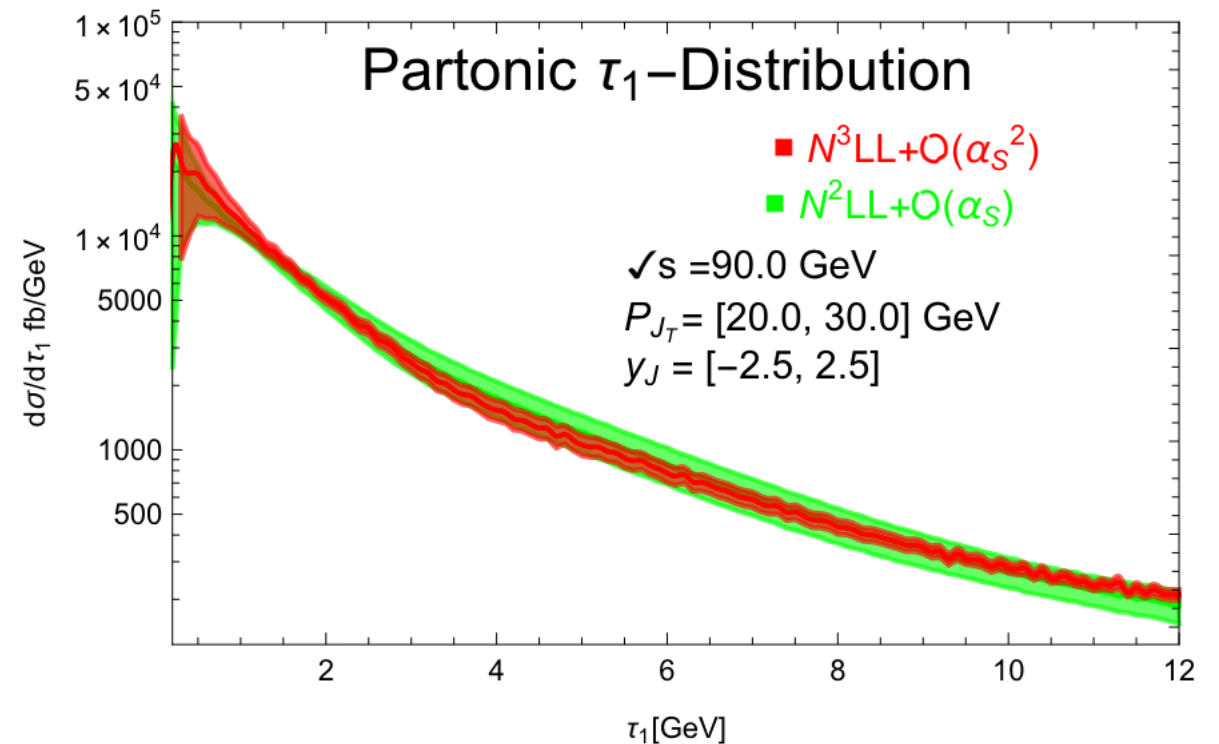
The process is primarily sensitive to the initial state's broadening effects, thereby serving as a clean probe of nTMD PDF

Precision calculation for jets in DIS

- Precision calculations in DIS are essential for enhancing our understanding of partonic interactions and the internal structure of nucleons.
- The high-order calculation has reached N3LO accuracy for jet production in DIS [Currie, Gehrmann, Glover, Huss, Niehues, & Vogt '18](#)
- Several global event shape distributions in DIS are known at N3LL + $\mathcal{O}(\alpha_s^2)$
 - **thrust** [Kang, Lee, & Stewart '15](#)
 - **(transverse) energy energy correlator** [Li, Vitev, & Zhu '20, Li, Makris, Vitev '21](#)
 - **1-jettiness** [Cao, Kang, Liu & Mantry '23](#)



[Arratia, Kang, Prokudin, Ringer '19](#)



[Cao, Kang, Liu & Mantry '23](#)

N³LL + $\mathcal{O}(\alpha_s^2)$ predictions on lepton jet azimuthal correlation in DIS

Fang, Gao, Li, DYS 2407.XXXXX

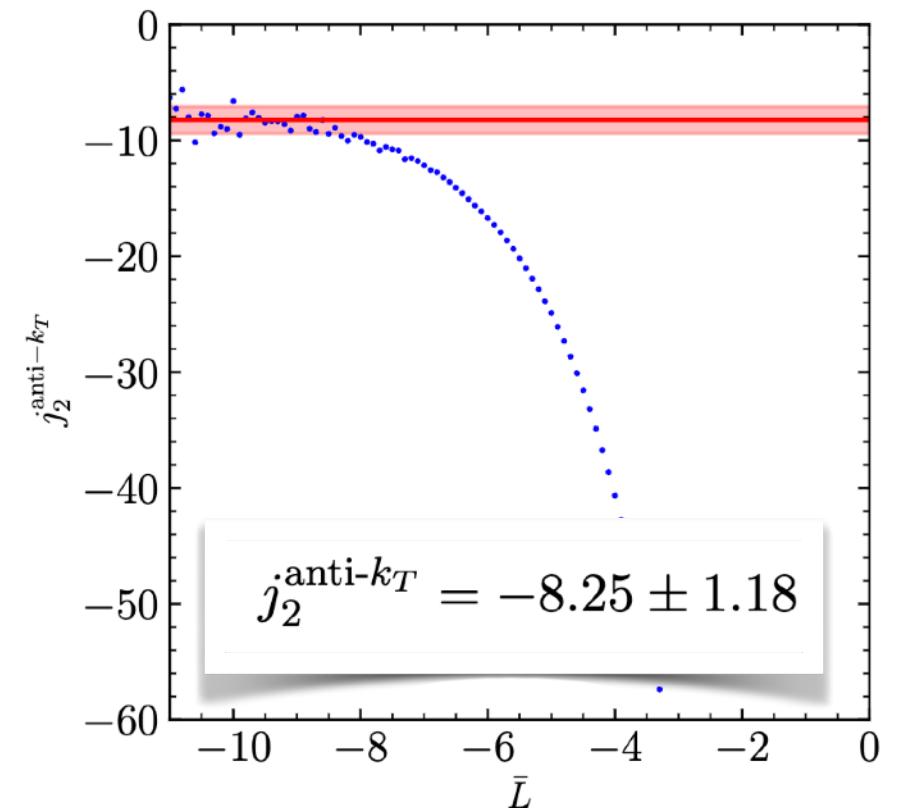
- All ingredients are known at N³LL+ $\mathcal{O}(\alpha_s^2)$, except the two loop jet function j_2 .
 - It was extracted numerically from the Event2 (Gutierrez-Reyes, Scimemi, Waalewijn, Zoppi '19)
 - A preliminary numerical results are also calculated from SoftSERVE (Brune SCET2023)
- We study dijet production in e+e-, and compare two-loop singular cross section and $\mathcal{O}(\alpha_s^2)$ predictions from NLOJET++ generator to extract j_2

$$\frac{d\sigma}{dq_T} = \bar{\sigma}_0 H(Q, \mu_h) q_T \int_0^\infty b_T db_T J_0(q_T b_T) J_q(b_T, \mu_h, \zeta_f) J_{\bar{q}}(b_T, \mu_h, \zeta_f)$$

Integrated cross section: $\sigma_L(Q_T) \equiv \int_0^{Q_T} dq_T \frac{d\sigma}{dq_T}$

Two-loop coefficient:

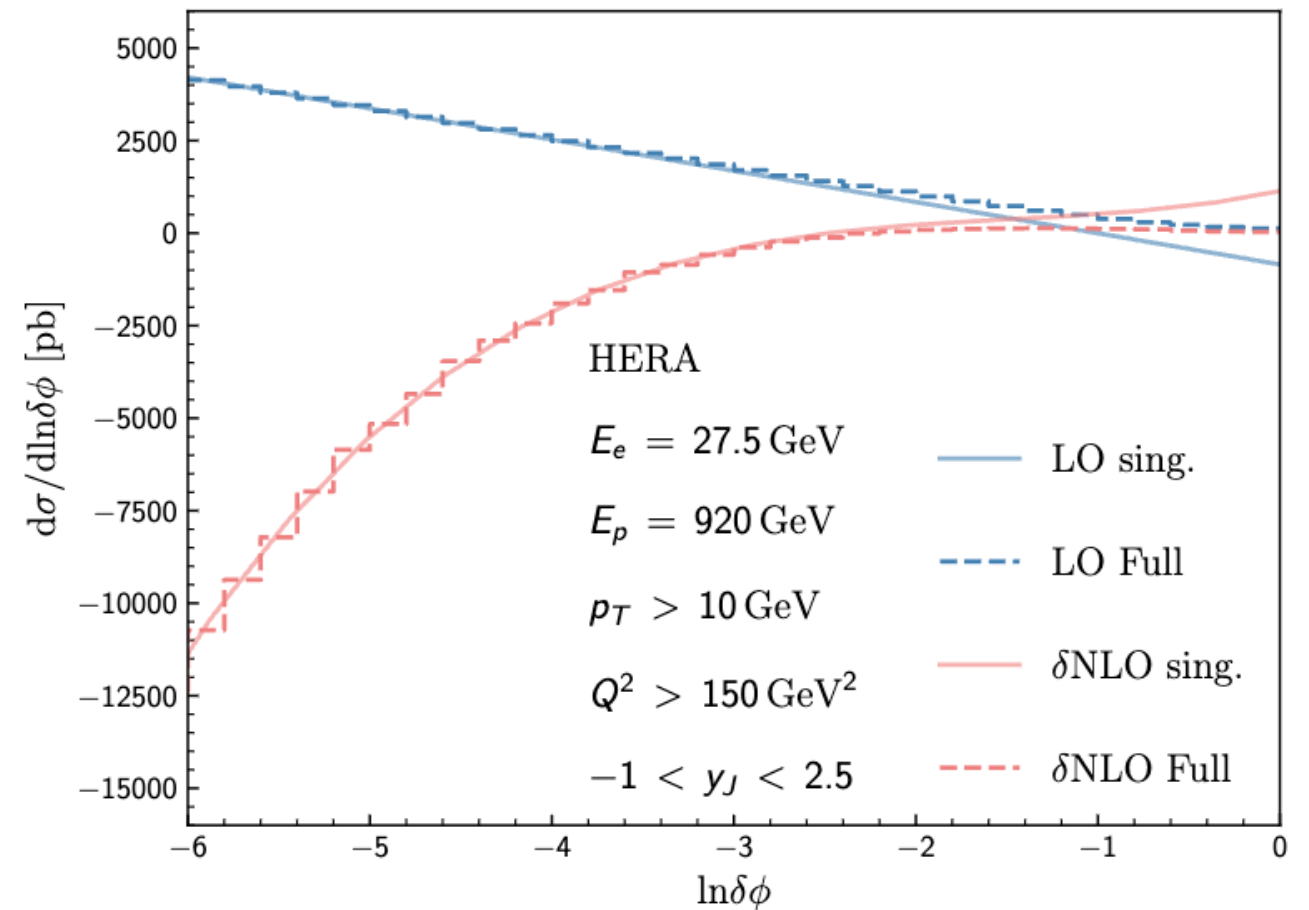
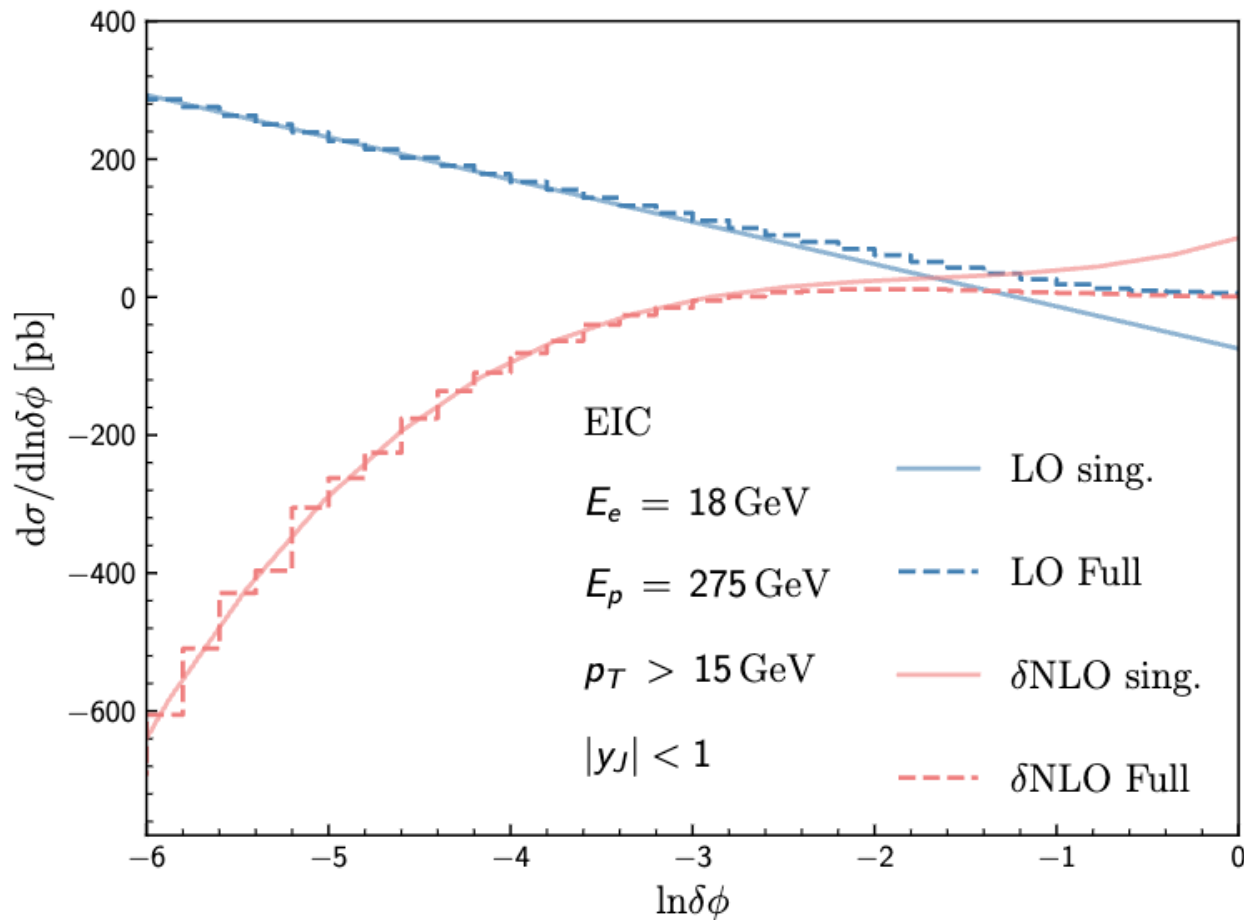
$$\begin{aligned}
 B = & C_F^2 \left[\frac{\bar{L}^4}{2} + 3\bar{L}^3 + \bar{L}^2 \left(\frac{11}{2} - \frac{\pi^2}{3} + 6 \ln 2 \right) + \bar{L} \left(\frac{9}{4} + 18 \ln 2 - 4 \zeta_3 \right) - \frac{189}{16} + 5 \pi^2 \right. \\
 & \left. - \frac{173 \pi^4}{720} + 27 \ln 2 - \frac{9}{2} \pi^2 \ln 2 + 9 \ln^2 2 - 3 \zeta_3 \right] + C_F C_A \left[\frac{11 \bar{L}^3}{9} + \bar{L}^2 \left(-\frac{35}{36} + \frac{\pi^2}{6} \right) \right. \\
 & \left. + \bar{L} \left(-\frac{57}{4} + \frac{11 \pi^2}{18} + 11 \ln 2 + 6 \zeta_3 \right) - \frac{51157}{1296} + \frac{1061 \pi^2}{216} - \frac{2 \pi^4}{45} + \frac{401 \zeta_3}{18} \right] \\
 & + C_F T_F n_f \left[-\frac{4 \bar{L}^3}{9} + \frac{\bar{L}^2}{9} + \bar{L} \left(5 - \frac{2 \pi^2}{9} - 4 \ln 2 \right) + \frac{4085}{324} - \frac{91 \pi^2}{54} - \frac{14 \zeta_3}{9} \right] \\
 & + \frac{j_2}{2},
 \end{aligned}$$



$N^3LL + \mathcal{O}(\alpha_s^2)$ predictions on lepton jet azimuthal correlation in DIS

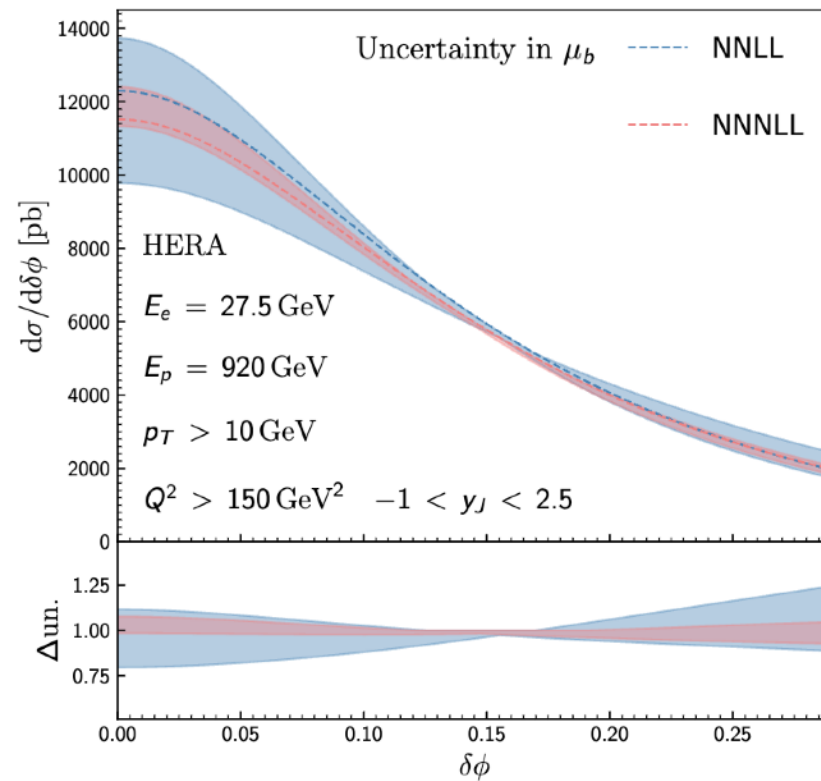
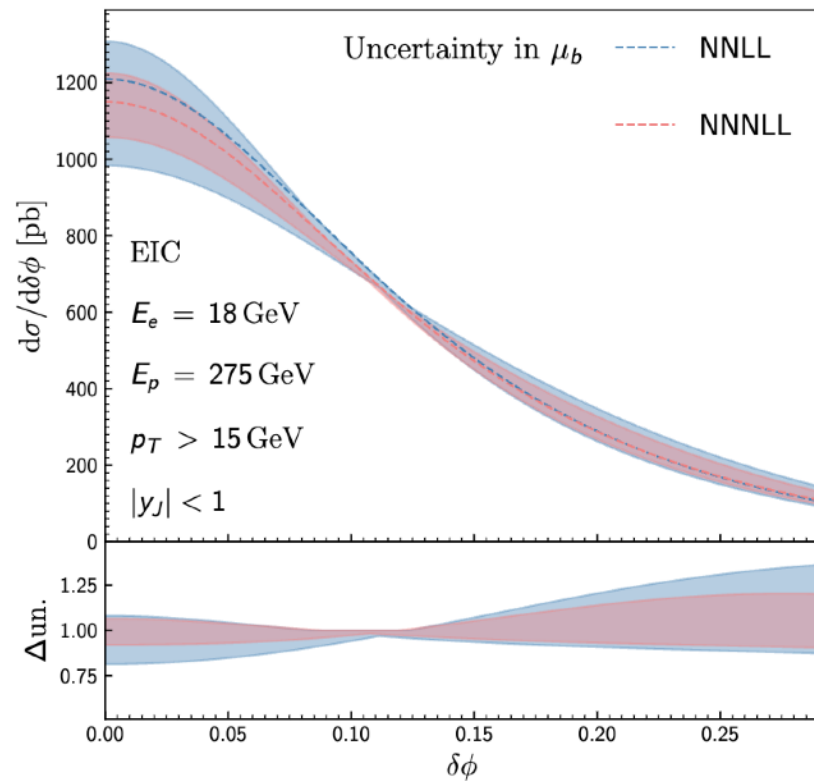
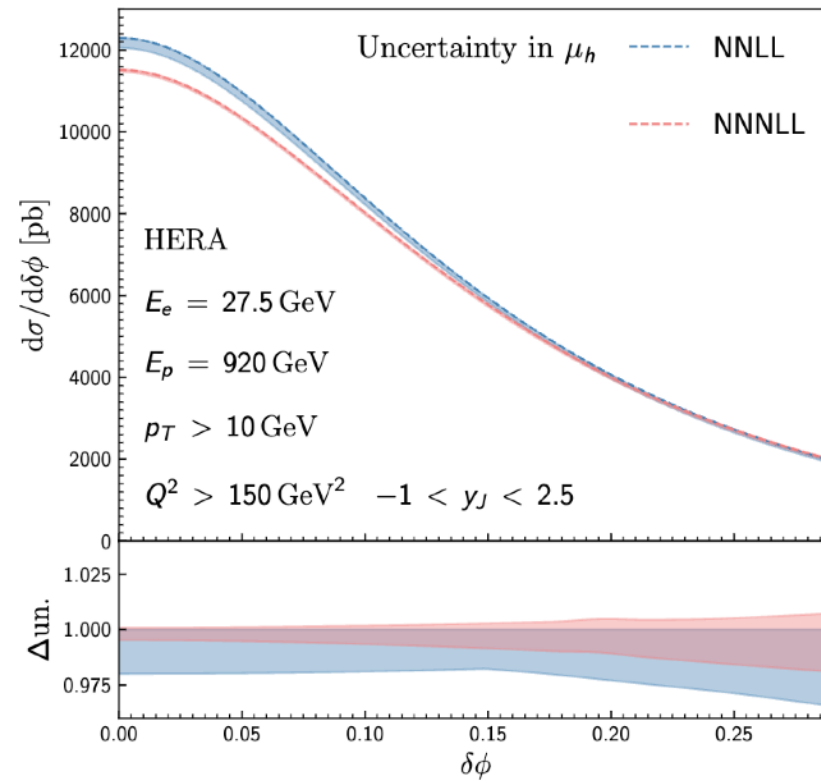
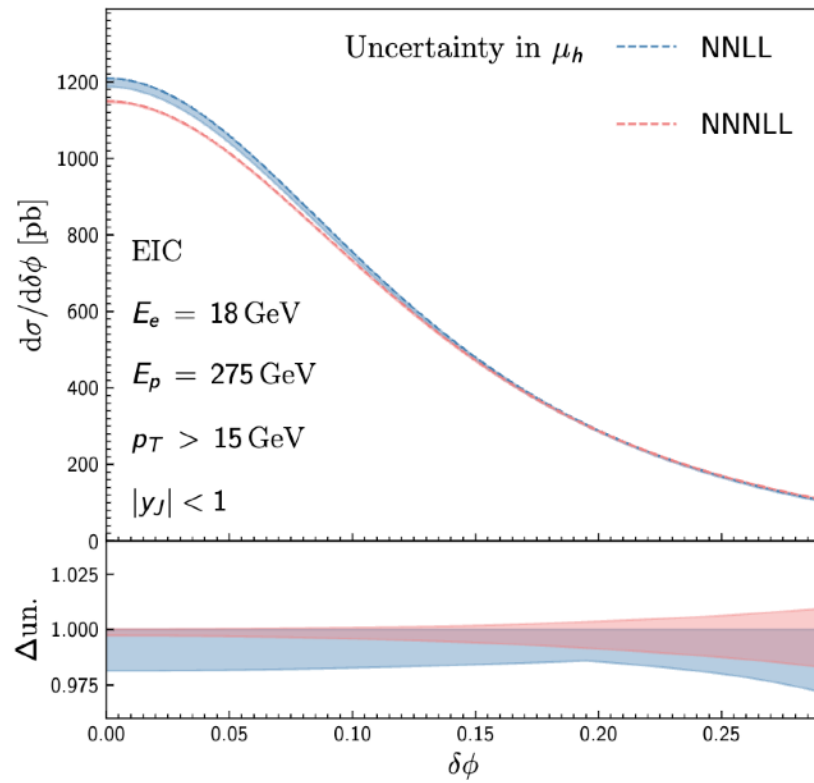
Fang, Gao, Li, DYS 2407.XXXXX

- We also compare the resummation expanded singular contribution in DIS with the full prediction from NLOJET++ up to $\mathcal{O}(\alpha_s^2)$.
- Good agreement in the back-to-back limit ($\delta\phi \rightarrow 0$) is observed.
- Matching corrections (Y term) are important in the large $\delta\phi$ region



Comparison of resummation results at N2LL and N3LL

Fang, Gao, Li, DYS 2407.XXXXX



- The uncertainty bands are narrower at N3LL (red) compared to NNLL (blue)

- At N3LL the dominant scale uncertainties are from μ_b variation

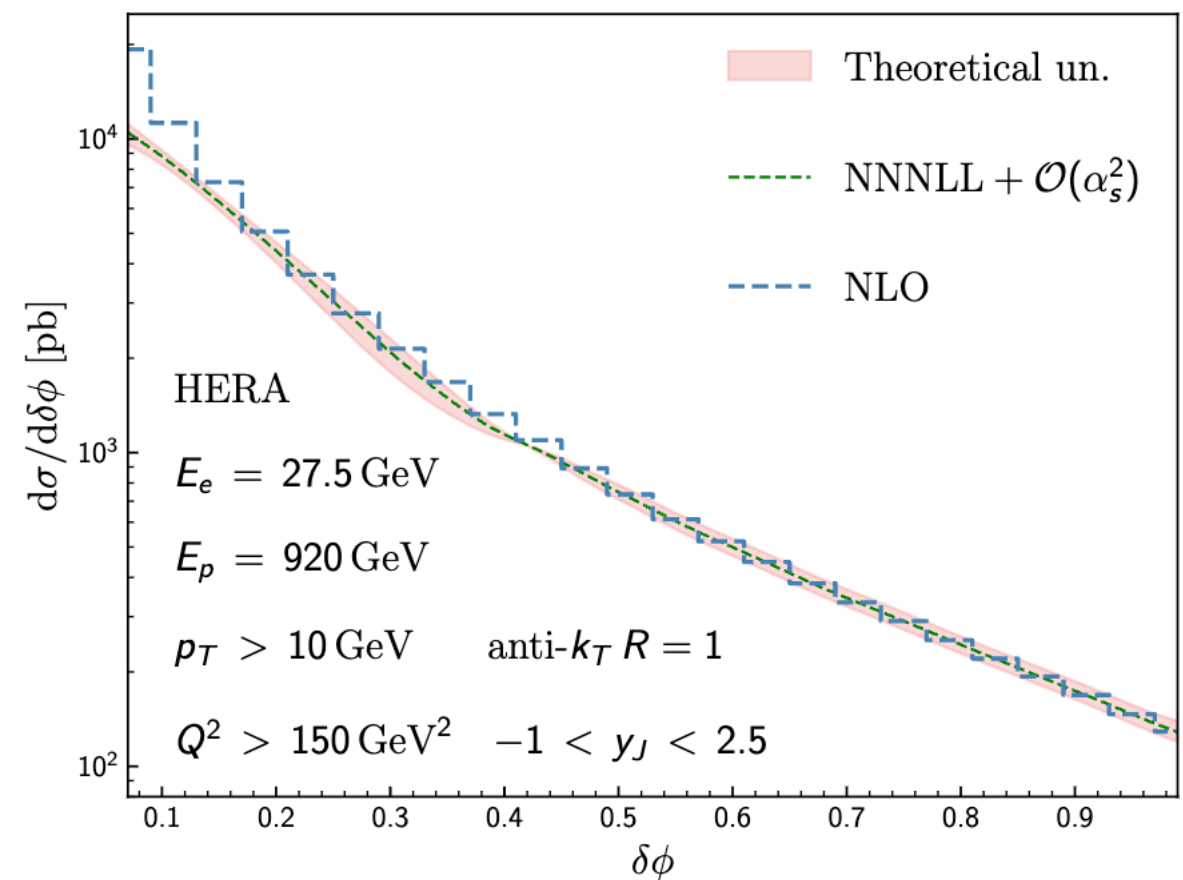
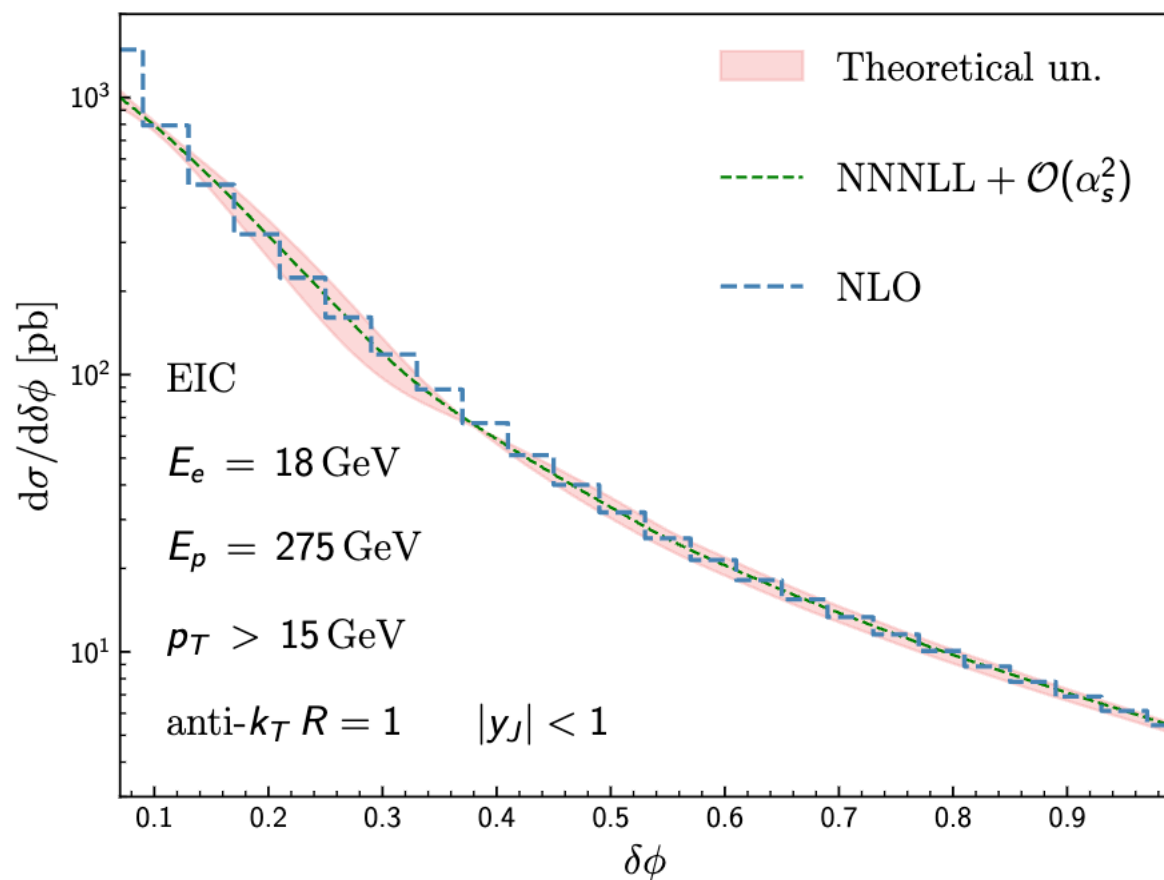
N³LL + $\mathcal{O}(\alpha_s^2)$ predictions on lepton jet azimuthal correlation in DIS

Fang, Gao, Li, DYS 2407.XXXXX

- In the large $\delta\phi$ region the resummation formula receives significant matching corrections
- It is necessary to switch off the resummation and instead employ fixed-order calculations

$$d\sigma_{\text{add}}(\text{NNNLL} + \mathcal{O}(\alpha_s^2)) \equiv d\sigma(\text{NNNLL}) + \underbrace{d\sigma(\text{NLO}) - d\sigma(\text{NLO singular})}_{d\sigma(\text{NLO non-singular})}$$

$$d\sigma(\text{NNNLL} + \mathcal{O}(\alpha_s^2)) = [1 - t(\delta\phi)]d\sigma_{\text{add}}(\text{NNNLL} + \mathcal{O}(\alpha_s^2)) + t(\delta\phi)d\sigma(\text{NLO})$$



Probing transverse momentum dependent structures with azimuthal dependence of energy correlators

Kang, Lee, DYS, Zhao JHEP03(2024)153

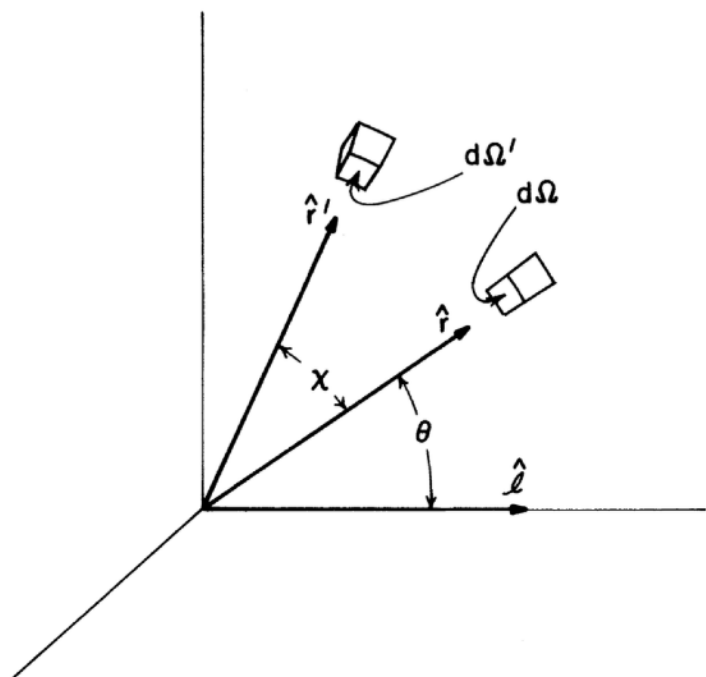
EEC in e+e-

Louis Basham, Brown, Ellis, & Love '78

$$\frac{d^2\Sigma}{d\Omega d\Omega'} = \frac{\alpha^2}{4W^2} \sum_f 3Q_f^2 \frac{\bar{g}_W^2}{3\pi^2} \frac{1}{32\pi} \frac{1}{1-\zeta} \left\{ \left[\left(\frac{36}{\zeta^5} - \frac{96}{\zeta^4} + \frac{72}{\zeta^3} - \frac{16}{\zeta^2} \right) \ln(1-\zeta) + \frac{36}{\zeta^4} - \frac{78}{\zeta^3} + \frac{36}{\zeta^2} \right] (1 + \cos^2\theta) \right.$$

$$+ 4\zeta(1-\zeta) \left[\left(\frac{6}{\zeta^5} - \frac{8}{\zeta^4} \right) \ln(1-\zeta) + \frac{6}{\zeta^4} - \frac{5}{\zeta^3} - \frac{2}{\zeta^2} \right] [\cos^2\varphi - \cos^2\theta (1 + \cos^2\varphi)]$$

$$\left. + 2[\zeta(1-\zeta)]^{1/2} \left[\left(-\frac{36}{\zeta^5} + \frac{72}{\zeta^4} - \frac{40}{\zeta^3} \right) \ln(1-\zeta) - \frac{36}{\zeta^4} + \frac{54}{\zeta^3} - \frac{16}{\zeta^2} - \frac{8}{\zeta} \right] \cos\theta \sin\theta \cos\varphi \right\}.$$



↓ $\int d\varphi$

$$\sigma_{\text{tot}} \frac{\bar{g}_W^2}{4\pi^2} \frac{3}{16\pi} [A(\zeta) + \cos^2\theta B(\zeta)]$$

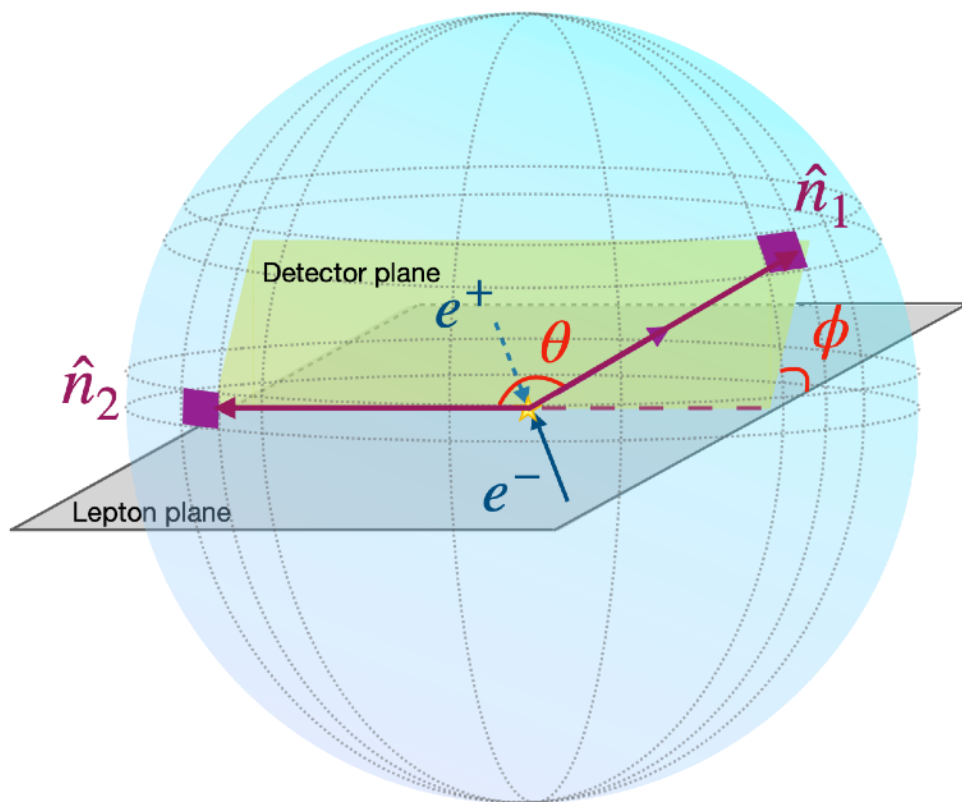
Perturbative coefficients:

$$A(\zeta) = \frac{1}{6(1-\zeta)} \left[\left(\frac{18}{\zeta^5} - \frac{42}{\zeta^4} + \frac{22}{\zeta^3} \right) \ln(1-\zeta) + \frac{18}{\zeta^4} - \frac{33}{\zeta^3} + \frac{7}{\zeta^2} + \frac{3}{\zeta} + 2 \right],$$

$$B(\zeta) = \frac{1}{6(1-\zeta)} \left[\left(\frac{18}{\zeta^5} - \frac{66}{\zeta^4} + \frac{78}{\zeta^3} - \frac{32}{\zeta^2} \right) \ln(1-\zeta) + \frac{18}{\zeta^4} - \frac{57}{\zeta^3} + \frac{51}{\zeta^2} - \frac{9}{\zeta} - 6 \right],$$

Spin asymmetry of EEC in the large angle limit

- Many spin asymmetries arise from the azimuthal correlations
- Azimuthal angle dependence in the small angle limit [Chen, Moult, & Zhu '20](#); [Li, Liu, Yuan, Zhu '23](#)
- We extend the EEC in the back-to-back by considering azimuthal asymmetries associated with the EEC [Kang, Lee, DYS, Zhao '23](#)



$$\frac{1}{\sigma_{\text{tot}}} \frac{d\Sigma_{e^+e^-}}{d\tau d\phi} = \frac{\langle \mathcal{O} \mathcal{E}(\vec{n}_1) \mathcal{E}(\vec{n}_2) \mathcal{O}^\dagger \rangle}{\langle \mathcal{O} \mathcal{O}^\dagger \rangle}$$

$$\text{EEC}_{e^+e^-}(\tau, \phi) \equiv \frac{d\Sigma_{e^+e^-}}{d\tau d\phi} = \frac{1}{2} \sum_{1,2} \int d\sigma z_1 z_2 \delta\left(\tau - \frac{1 + \cos\theta_{12}}{2}\right) \delta(\phi - \phi_{12})$$

Azimuthal dependent EEC in e^+e^-

- The standard TMD factorization for the back-to-back di-hadron process

$$\frac{d\sigma}{dz_i dz_j d^2\mathbf{q}_T} = \sigma_0 H(Q, \mu) \sum_q e_q^2 \int d^2\mathbf{p}_{1\perp} d^2\mathbf{p}_{2\perp} d^2\boldsymbol{\lambda}_\perp \delta^2\left(\frac{\mathbf{p}_{1\perp}}{z_1} + \frac{\mathbf{p}_{2\perp}}{z_2} - \boldsymbol{\lambda}_\perp + \mathbf{q}_T\right) S(\boldsymbol{\lambda}_\perp^2, \mu, \nu)$$

$$\times \left[D_{1,h_1/q}^{(u)}(z_1, \mathbf{p}_{1\perp}^2, \mu, \zeta/\nu^2) D_{1,h_2/\bar{q}}^{(u)}(z_2, \mathbf{p}_{2\perp}^2, \mu, \zeta/\nu^2) + \cos(2\phi_{12}) \left(\hat{\mathbf{q}}_{T,\alpha} \hat{\mathbf{q}}_{T,\beta} - \frac{1}{2} g_{\perp,\alpha\beta} \right) \right.$$

$$\left. \times \frac{\mathbf{p}_{1\perp}^\alpha}{z_1 M_1} H_{1,h_1/q}^{\perp(u)}(z_1, \mathbf{p}_{1\perp}^2, \mu, \zeta/\nu^2) \frac{\mathbf{p}_{2\perp}^\beta}{z_2 M_2} H_{1,h_2/\bar{q}}^{\perp(u)}(z_2, \mathbf{p}_{2\perp}^2, \mu, \zeta/\nu^2) \right].$$

$$z_i = \frac{2P_{hi} \cdot q}{Q^2} = \frac{2E_i}{Q}$$

Energy fraction

$$D_{1,h/q}^{(u)}(z, \mathbf{p}_\perp^2, \mu, \zeta/\nu^2)$$

Unpolarized TMD FF

$$H_{1,h/q}^{\perp(u)}(z, \mathbf{p}_\perp^2, \mu, \zeta/\nu^2)$$

Collins TMD FF

Leading Quark TMDFFs



		Quark Polarization		
		Un-Polarized (U)	Longitudinally Polarized (L)	Transversely Polarized (T)
Polarized Hadrons	Γ		$G_1 = \begin{array}{c} \text{---} \text{---} \text{---} \\ \text{---} \end{array}$ Helicity	$H_{1L}^\perp = \begin{array}{c} \text{---} \text{---} \end{array}$
	T	$D_{1T}^\perp = \begin{array}{c} \uparrow \\ \text{---} \end{array} - \begin{array}{c} \downarrow \\ \text{---} \end{array}$ Polarizing FF	$G_{1T}^\perp = \begin{array}{c} \uparrow \\ \text{---} \end{array} - \begin{array}{c} \uparrow \\ \text{---} \end{array}$	$H_1 = \begin{array}{c} \uparrow \\ \text{---} \end{array} - \begin{array}{c} \uparrow \\ \text{---} \end{array}$ Transversity $H_{1T}^\perp = \begin{array}{c} \uparrow \\ \text{---} \end{array} - \begin{array}{c} \uparrow \\ \text{---} \end{array}$
Unpolarized (or Spin 0) Hadrons		$D_1 = \begin{array}{c} \text{---} \\ \bullet \end{array}$ Unpolarized		$H_1^\perp = \begin{array}{c} \uparrow \\ \text{---} \end{array} - \begin{array}{c} \uparrow \\ \text{---} \end{array}$ Collins

Azimuthal dependent EEC in e^+e^-

- The TMD factorization for the azimuthal-dependent EEC in the back-to-back limit

$$\text{EEC}_{e^+e^-}(\tau, \phi) = \frac{1}{2}\sigma_0 H(Q, \mu) \sum_q e_q^2 \int \frac{b db}{2\pi} \left[J_0(b\sqrt{\tau}Q) J_q(b, \mu, \zeta) J_{\bar{q}}(b, \mu, \zeta) + \cos(2\phi) \frac{b^2}{8} J_2(b\sqrt{\tau}Q) J_q^\perp(b, \mu, \zeta) J_{\bar{q}}^\perp(b, \mu, \zeta) \right]$$

New term: azimuthal asymmetry
 “Collins-type” EEC jet functions

A similar structure for Winner-take-All jet function was given in W. Lai, X. Liu, M Wang, H. Xing '21 '22

- The unpolarized EEC jet function has a close relation to the unpolarized TMD FFs

$$J_q(b, \mu, \zeta) \equiv \sum_h \int_0^1 dz z \tilde{D}_{1,h/q}(z, b, \mu, \zeta)$$

- Collins-type EEC jet functions are closely connected with the Collins FFs

$$J_q^\perp(b, \mu, \zeta) \equiv \sum_h \int_0^1 dz z \tilde{H}_{1,h/q}^\perp(z, b, \mu, \zeta)$$

Collins-type EEC jet function

- We introduce Collins-type EEC jet function

$$J_q(\mathbf{b}, \mu, \zeta) \equiv \sum_h \int_0^1 dz z \tilde{D}_{1,h/q}(z, b, \mu_{b_*}, \zeta_i) e^{-S_{\text{pert}}(\mu, \mu_{b_*}) - S_{\text{NP}}^{D_1}(b, Q_0, \zeta)} \left(\sqrt{\frac{\zeta}{\zeta_i}} \right)^{\kappa(b, \mu_{b_*})}$$

$$J_q^\perp(\mathbf{b}, \mu, \zeta) \equiv \sum_h \int_0^1 dz z \tilde{H}_{1,h/q}^\perp(z, b, \mu_{b_*}, \zeta_i) e^{-S_{\text{pert}}(\mu, \mu_{b_*}) - S_{\text{NP}}^{H_1^\perp}(b, Q_0, \zeta)} \left(\sqrt{\frac{\zeta}{\zeta_i}} \right)^{\kappa(b, \mu_{b_*})}$$

Collins function in b -space

- The OPE of the subtracted unpolarized and Collins TMD FFs gives

$$\tilde{D}_{1,h/q}(z, b, \mu, \zeta) = [C_{j \leftarrow q} \otimes D_{1,h/j}](z, b, \mu, \zeta) + \mathcal{O}(b^2 \Lambda_{\text{QCD}}^2),$$

$$\tilde{H}_{1,h/q}^\perp(z, b, \mu, \zeta) = [\delta C_{j \leftarrow q}^{\text{Collins}} \otimes \hat{H}_{1,h/j}^{\perp(3)} + A_{j \leftarrow q} \otimes \hat{H}_{F,h/j}](z, b, \mu, \zeta) + \mathcal{O}(b^2 \Lambda_{\text{QCD}}^2),$$

twist-3 FFs (H_F is ignored)

$$\delta C_{q' \leftarrow q}^{\text{Collins}}(z, b, \mu, \zeta) = \delta_{qq'} \left\{ \delta(1-z) + \frac{\alpha_s}{\pi} \left[C_F \delta(1-z) \left(-\frac{L_b^2}{4} + \frac{L_b}{2} \left(\frac{3}{2} + \ln \frac{\mu^2}{\zeta^2} \right) - \frac{\pi^2}{24} \right) \right. \right. \\ \left. \left. + \left(\ln z - \frac{L_b}{2} \right) \hat{P}_{q \leftarrow q}^c(z) \right] \right\} + \mathcal{O}(\alpha_s^2),$$

The OPE of the Collins TMD FFs

- The OPE of the subtracted unpolarized and Collins TMD FFs gives

$$\tilde{H}_{1,h/q}^\perp(z, b, \mu, \zeta) = \left[\delta C_{j \leftarrow q}^{\text{Collins}} \otimes \hat{H}_{1,h/j}^{\perp(3)} + A_{j \leftarrow q} \tilde{\otimes} \hat{H}_{F,h/j} \right] (z, b, \mu, \zeta) + \mathcal{O}(b^2 \Lambda_{\text{QCD}}^2)$$

- **Standard convolution** $\left[C_{j \leftarrow q} \otimes F_{h/j} \right] (z, b, \mu, \zeta) = \int_z^1 \frac{dx}{x} C_{j \leftarrow q} \left(\frac{z}{x}, b, \mu, \zeta \right) F_{h/j} (x, \mu)$

$$\delta C_{q' \leftarrow q}^{\text{Collins}} (z, b, \mu, \zeta) = \delta_{qq'} \left\{ \delta(1-z) + \frac{\alpha_s}{\pi} \left[C_F \delta(1-z) \left(-\frac{L_b^2}{4} + \frac{L_b}{2} \left(\frac{3}{2} + \ln \frac{\mu^2}{\zeta^2} \right) - \frac{\pi^2}{24} \right) + \left(\ln z - \frac{L_b}{2} \right) \hat{P}_{q \leftarrow q}^c(z) \right] \right\} + \mathcal{O}(\alpha_s^2),$$

$\hat{H}_{1,h/j}^{\perp(3)}(z, \mu)$: twist-3 fragmentation function, related to the first k_\perp -moment of the Collins TMD FF

- **Double convolution**

$$\left[A_{j \leftarrow q} \tilde{\otimes} \hat{H}_{F,h/j} \right] (z, b, \mu, \zeta) = \int_z^1 \frac{dx}{x} \int \frac{dz_1}{z_1^2} \text{PV} \left(\frac{1}{\frac{1}{x} - \frac{1}{z_1}} \right) A_{j \leftarrow q} \left(\frac{z}{x}, z_1, b, \mu, \zeta \right) \hat{H}_{F,h/j} (x, z_1, \mu)$$

starts at the order $\mathcal{O}(\alpha_s)$ and is ignored in our work

Sum rule

- The collinear functions in the OPE matching obey the sum rules

$$\sum_h \int_0^1 dz z D_{1,h/j}(z, \mu) = 1, \quad \text{sum over longitudinal momentum fraction carried by the hadron is 1}$$

$$\sum_h \int_0^1 dz \hat{H}_{1,h/q}^{\perp(3)}(z, \mu) = 0. \quad \text{the transverse momentum carried by the final hadron sum to 0 (Schafer-Teryaev sum rule)}$$

- In the OPE region $J_q^\perp(b, \mu, \zeta) = \sum_h \int_0^1 dz z \tilde{H}_{1,h/q}^\perp(z, b, \mu, \zeta)$

$$= \sum_h \int_0^1 dz \int_z^1 \frac{dx}{x} \delta C_{q \leftarrow q}^{\text{Collins}}\left(\frac{z}{x}, b, \mu_{b_*}, \zeta\right) \hat{H}_{1,h/q}^{\perp(3)}(x, \mu_{b_*}) e^{-S_{\text{pert}}(\mu, \mu_{b_*})}$$

$$= \int_0^1 d\tau \delta C_{q \leftarrow q}^{\text{Collins}}(\tau, b, \mu_{b_*}, \zeta) \left[\sum_h \int_0^1 dx \hat{H}_{1,h/q}^{\perp(3)}(x, \mu_{b_*}) \right] e^{-S_{\text{pert}}(\mu, \mu_{b_*})}$$

$$= 0, \quad \quad \quad = 0$$

- We find that the Collins-type EEC jet function becomes **zero in the OPE region** upon neglecting the off-diagonal matching terms.

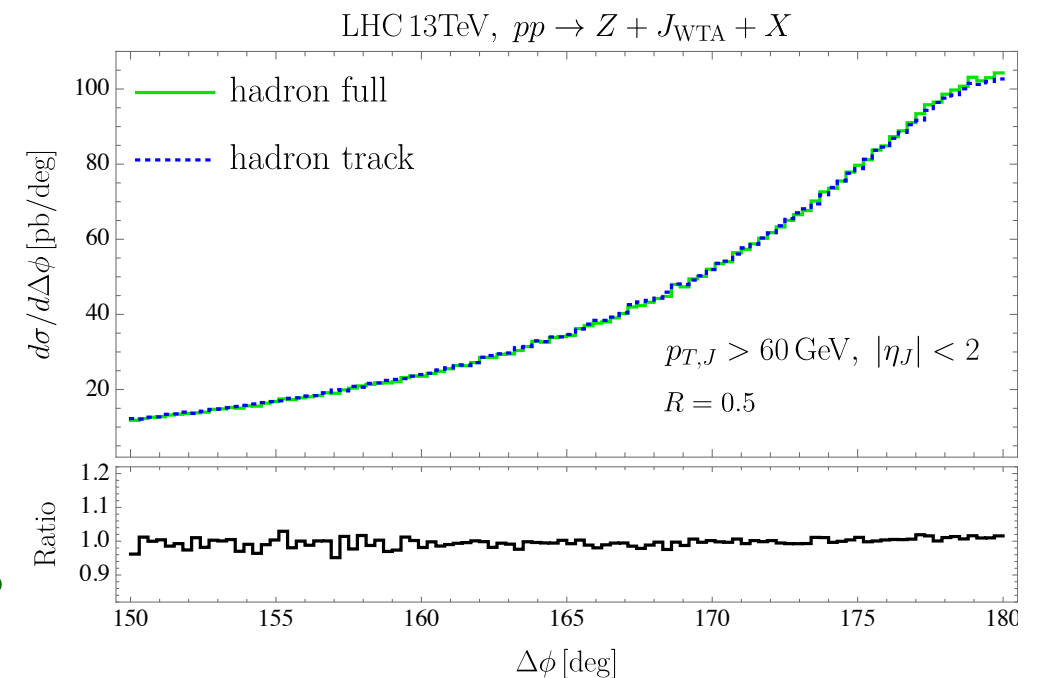
Collins-type EEC with subsets of hadrons

- In the small angle limit, the track function formalism was used to study energy correlation between hadrons with specific quantum number $\langle \mathcal{E}_{\mathcal{S}_1}(\hat{n}_1) \mathcal{E}_{\mathcal{S}_2}(\hat{n}_2) \rangle$ Chang, Procura, Thaler, & Waalewijn '13; Y, Li, Moult, Schrijnder, Waalewijn, H. X. Zhu '21; Jaarsma, Y. Li, Moult, Waalewijn, Z. X. Zhua '22, '23 + H. Chen '22 '23
- In the large angle limit (TMD region), one can also use subset \mathcal{S} of hadrons to define the jet function

- E.g. Tacking jet function for the recoil free jets

$$\bar{\mathcal{J}}_q^{(1)} = \mathcal{J}_q^{(1)} + 4C_F \int_0^1 dx \frac{1+x^2}{1-x} \ln \frac{x}{1-x} \int_0^1 dz_1 T_q(z_1, \mu) \times \int_0^1 dz_2 T_g(z_2, \mu) [\theta(z_1 x - z_2(1-x)) - \theta(x - \frac{1}{2})]$$

Chien, Rahn, DYS, Waalewijn & Wu '22 JHEP + Schrignder '21 PLB



- We explore a less inclusive version of EEC in the back-to-back limit that is only sensitive to the energy flow of subset \mathcal{S} of hadrons

$$\sum_h \Rightarrow \sum_{h \in \mathcal{S}}$$

E.g. $\mathcal{S} = \text{charged particles}$

Better energy resolution and smaller experimental uncertainties

$$\mathcal{S} = h$$

Probe fragmentation function

Collins-type EEC with subsets of hadrons

- We define the modified jet functions

$$J_{q/\mathbb{S}}(b, \mu, \zeta) \equiv \sum_{h \in \mathbb{S}} \int_0^1 dz z \tilde{D}_{1,h/q}(z, b, \mu, \zeta),$$

$$J_{q/\mathbb{S}}^\perp(b, \mu, \zeta) \equiv \sum_{h \in \mathbb{S}} \int_0^1 dz z \tilde{H}_{1,h/q}^\perp(z, b, \mu, \zeta).$$

- In the OPE region

$$F_{j \rightarrow \mathbb{S}} = \sum_{h \in \mathbb{S}} \int_0^1 dz z D_{1,h/j}(z, \mu_{b_*}) \quad \text{average fraction of longitudinal momentum carried by } \mathbb{S}$$

$$J_{q/\mathbb{S}}(b, \mu, \zeta) = \sum_j F_{j \rightarrow \mathbb{S}} \int_0^1 d\tau \tau C_{j \leftarrow q}(\tau, b, \mu_{b_*}, \zeta) e^{-S_{\text{pert}}(\mu, \mu_{b_*})},$$

$$J_{q/\mathbb{S}}^\perp(b, \mu, \zeta) = \sum_j F_{j \rightarrow \mathbb{S}}^\perp \int_0^1 d\tau \delta C_{j \leftarrow q}^{\text{Collins}}(\tau, b, \mu_{b_*}, \zeta) e^{-S_{\text{pert}}(\mu, \mu_{b_*})}.$$

$$F_{j \rightarrow \mathbb{S}}^\perp = \sum_{h \in \mathbb{S}} \int_0^1 dz \hat{H}_{1,h/j}^{\perp(3)}(z, \mu_{b_*}) \quad \text{average transverse momentum carried by } \mathbb{S}$$

- All the non-perturbative information are captured by the moments of FFs in the OPE region

Collins-type EEC with subsets of hadrons

- From the perspective of Collins-type EEC jet function, we are motivated to consider the so-called favored and unfavored subset

- Twist-3 Collins fragmentation functions

$$\hat{H}_{\pi^+/\bar{u}}^{(3)}(z, Q_0) = \hat{H}_{\pi^-/u}^{(3)}(z, Q_0) = \hat{H}_{\pi^-/\bar{d}}^{(3)}(z, Q_0) = \hat{H}_{\text{unf}}(z, Q_0),$$

$$\hat{H}_{\pi^+/\bar{d}}^{(3)}(z, Q_0) = \hat{H}_{\pi^-/d}^{(3)}(z, Q_0) = \hat{H}_{\pi^-/\bar{u}}^{(3)}(z, Q_0) = \hat{H}_{\text{fav}}(z, Q_0).$$

$$\hat{H}_{\text{fav}}^{(3)}(z, Q_0) = N_u^c z^{\alpha_u} (\tau)^{\beta_u} D_{1,\pi^+/u}(z, Q_0),$$

$$\hat{H}_{\text{unfav}}^{(3)}(z, Q_0) = N_d^c z^{\alpha_d} (\tau)^{\beta_d} D_{1,\pi^+/d}(z, Q_0),$$

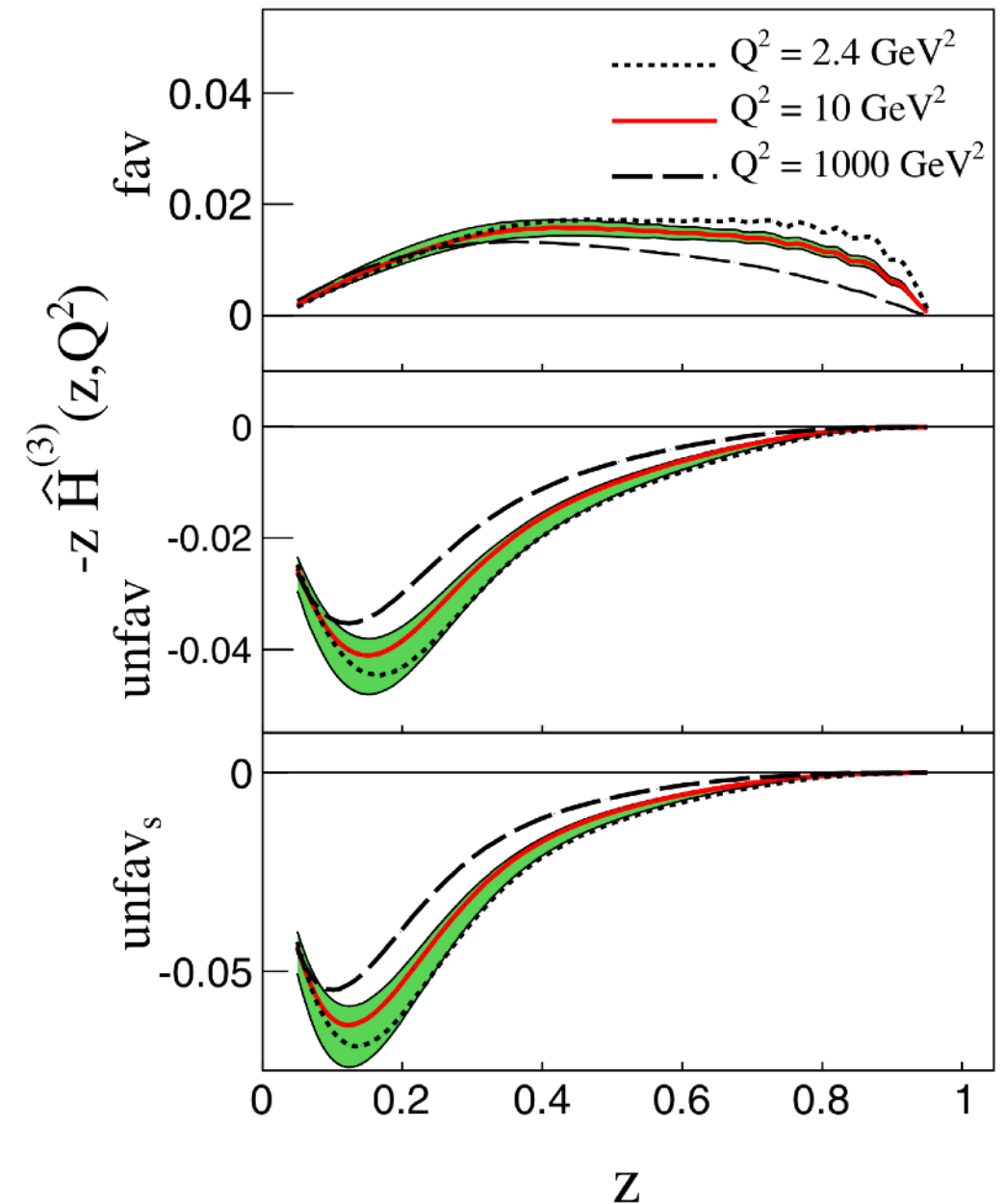
$$\hat{H}_{s/\bar{s}}^{(3)}(z, Q_0) = N_d^c z^{\alpha_d} (\tau)^{\beta_d} D_{1,\pi^+/s,\bar{s}}(z, Q_0),$$

- The vanishing value of Collins-type EEC jet function in the OPE region can be understood as

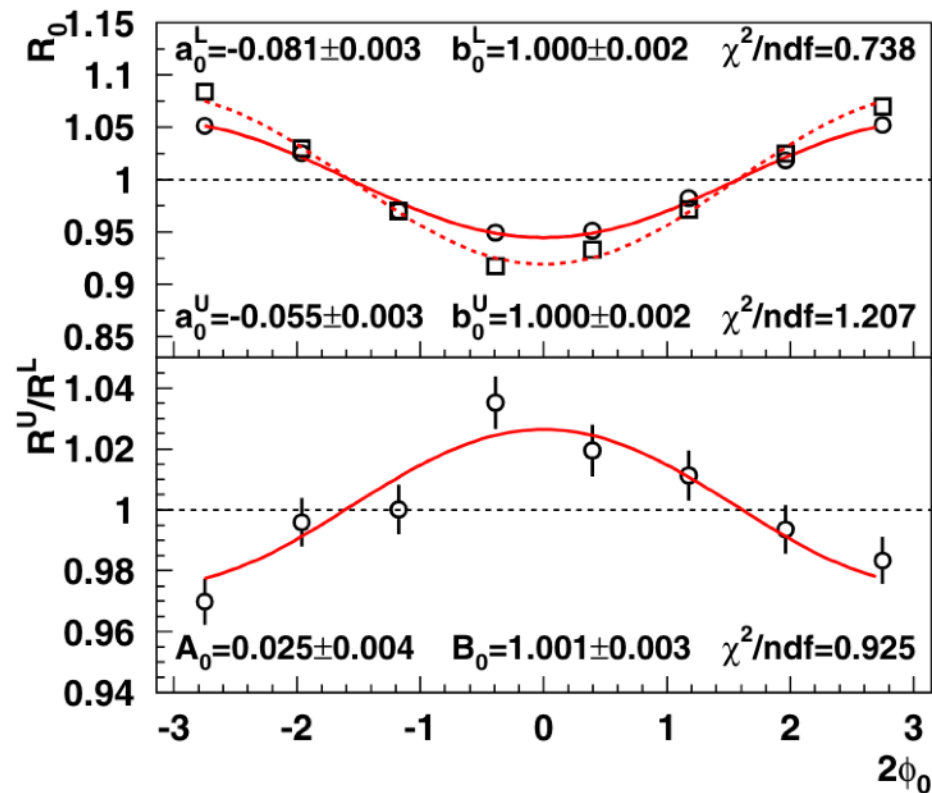
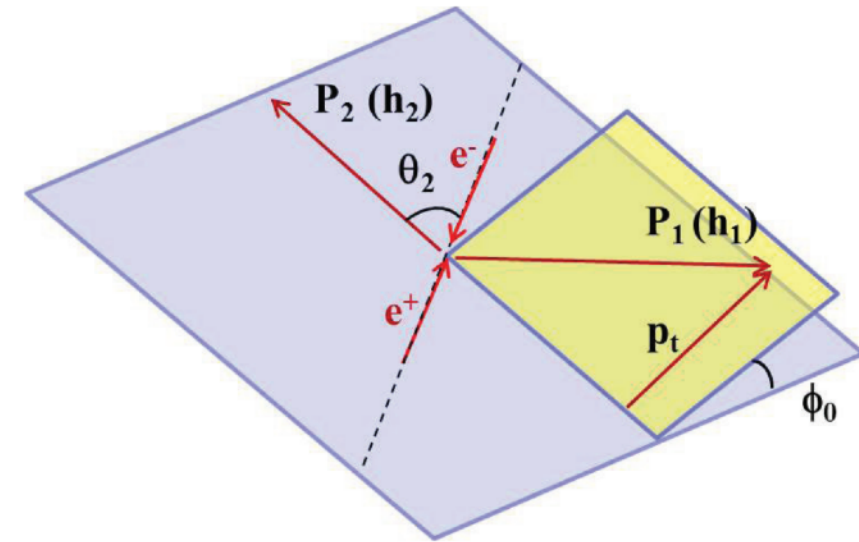
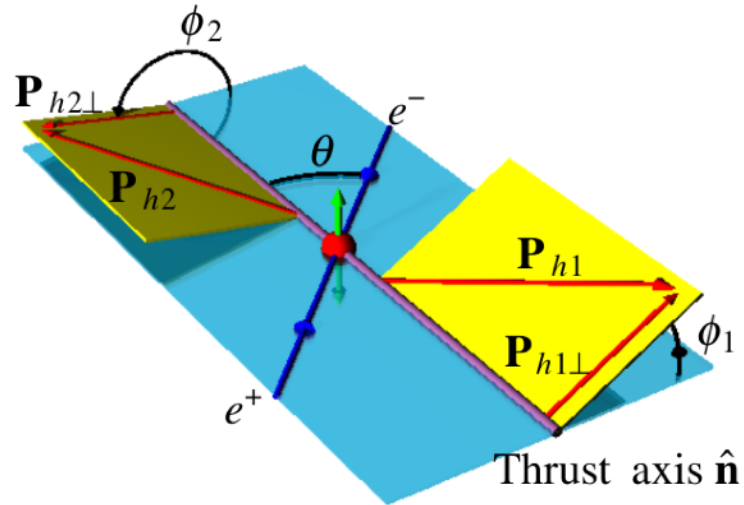
$$F_{j \rightarrow \text{fav}}^\perp \approx -F_{j \rightarrow \text{unfav}}^\perp$$

- In phenomenology we consider

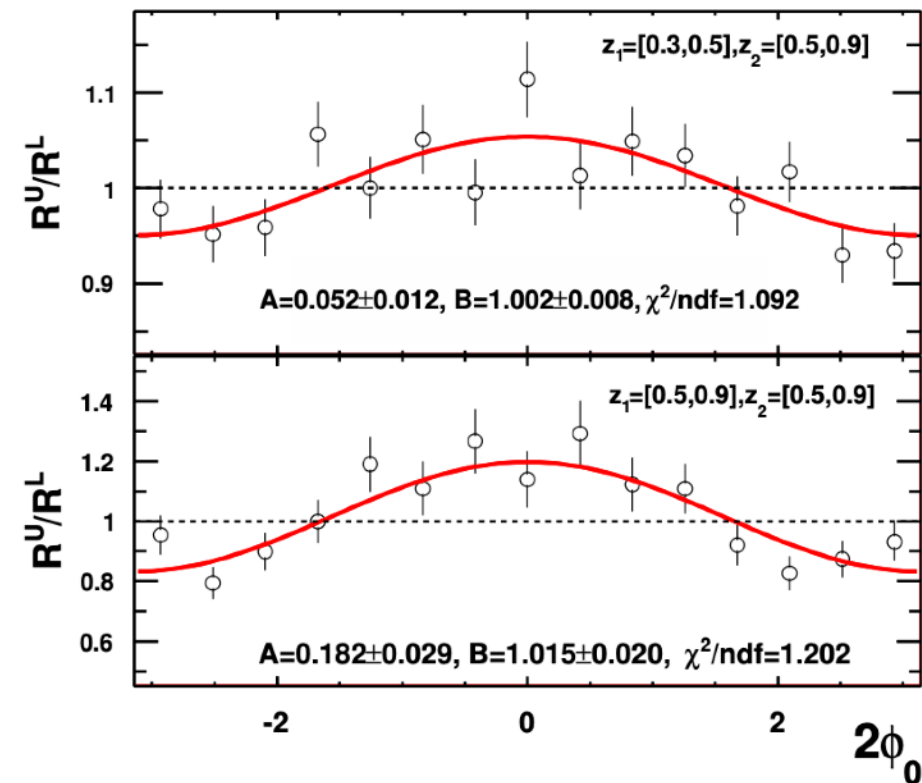
$$\mathbb{S} = \{\pi^+\}, \{\pi^-\}, \{\pi^0\}, \{\pi^+, \pi^-\}, \{\pi^+, \pi^-, \pi^0\}$$



Collins asymmetry in e^+e^-



Belle 2006

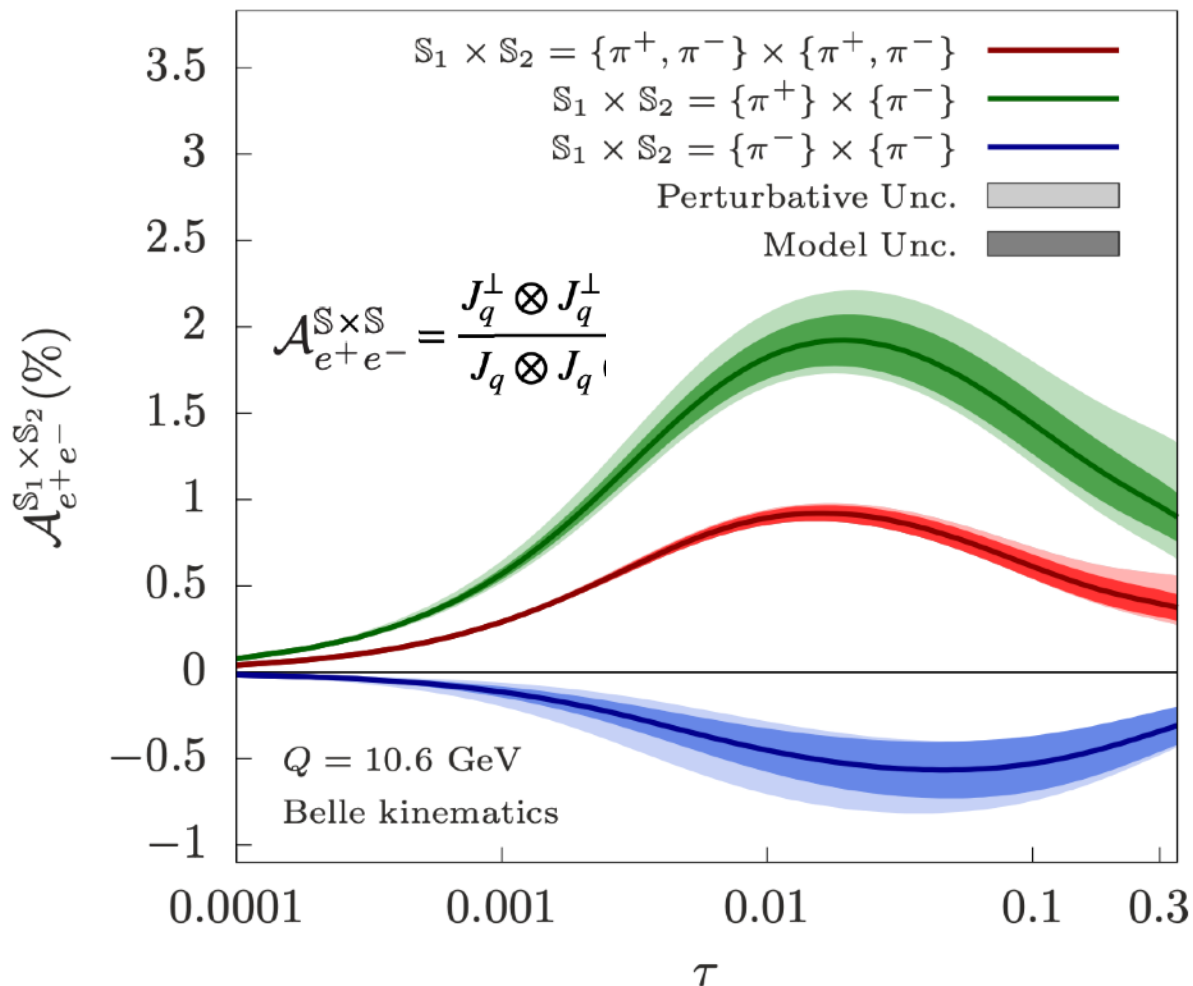


BESIII 2016

EEC in e^+e^- : Collins asymmetry

- We provide a prediction for Collins asymmetry at Belle kinematics

$$\begin{aligned} \text{EEC}_{e^+e^-}(\tau, \phi) &= \frac{d\Sigma_{e^+e^-}}{d\tau d\phi} = \frac{1}{2}\sigma_0 \sum_q e_q^2 \int d\mathbf{q}_T^2 \delta\left(\tau - \frac{\mathbf{q}_T^2}{Q^2}\right) Z_{uu} \left[1 + \cos(2\phi) \frac{Z_{\text{Collins}}}{Z_{uu}}\right] \\ &\equiv \frac{1}{2}\sigma_0 \sum_q e_q^2 Z_{uu} \left[1 + \cos(2\phi) A_{e^+e^-}(\tau Q^2)\right], \end{aligned}$$

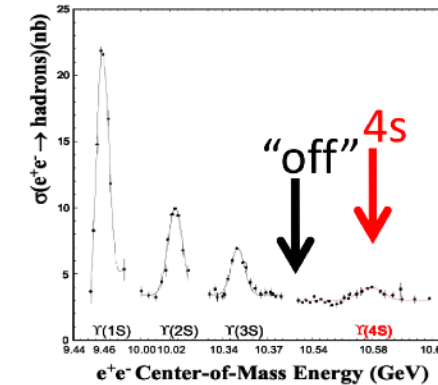
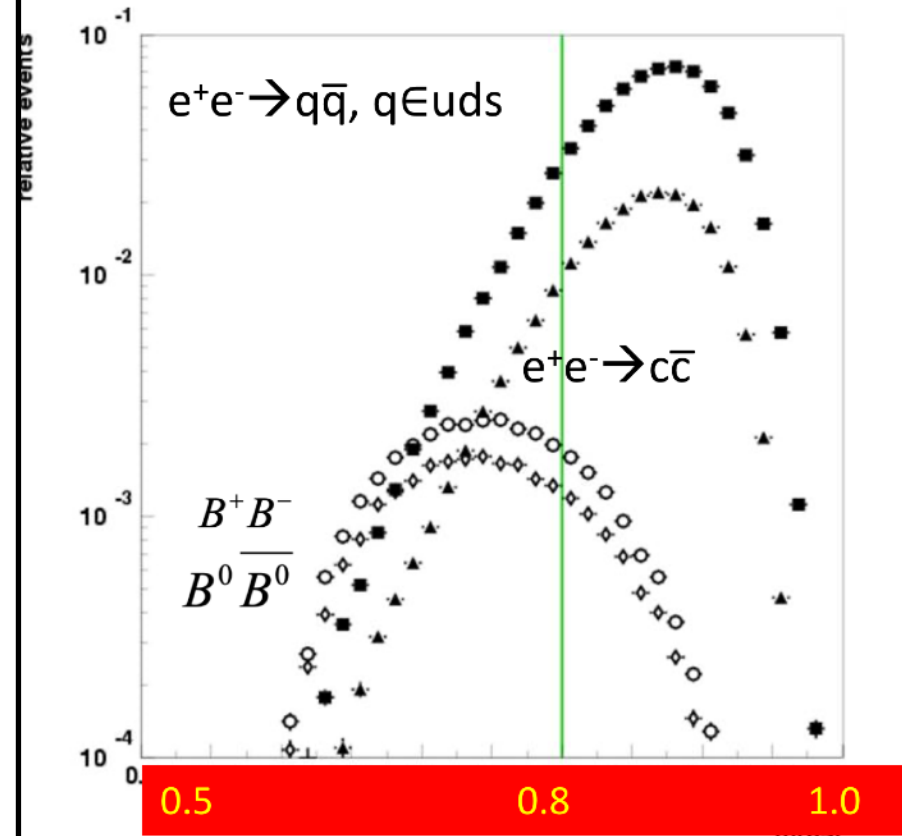


$$\begin{aligned} Z_{uu} &= \int \frac{bdb}{2\pi} J_0(bq_T) J_q(b, \mu, \zeta) J_{\bar{q}}(b, \mu, \zeta), \\ Z_{\text{Collins}} &= \int \frac{bdb}{2\pi} \frac{b^2}{8} J_2(bq_T) J_q^\perp(b, \mu, \zeta) J_{\bar{q}}^\perp(b, \mu, \zeta). \end{aligned}$$

- When choosing a subset of either positively or negatively charged pions detected in EEC, one observes sizable asymmetries, which worth further measurement.
- BESIII collaboration is performing this analysis

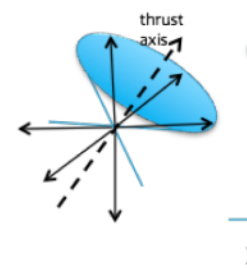
EEC at the Belle

Lots of data off resonance, easy to remove resonance background

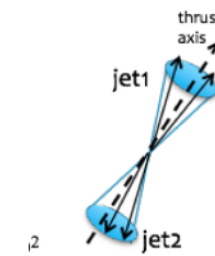


- small B contribution (<1%) in high thrust sample
- >75% of X-section continuum under $\Upsilon(4S)$ resonance
- $\sim 100 \text{ fb}^{-1} \rightarrow \sim 1000 \text{ fb}^{-1}$

$$\text{Thrust: } T = \frac{\sum_i |p_i \cdot \hat{n}|}{\sum_i |p_i|}$$



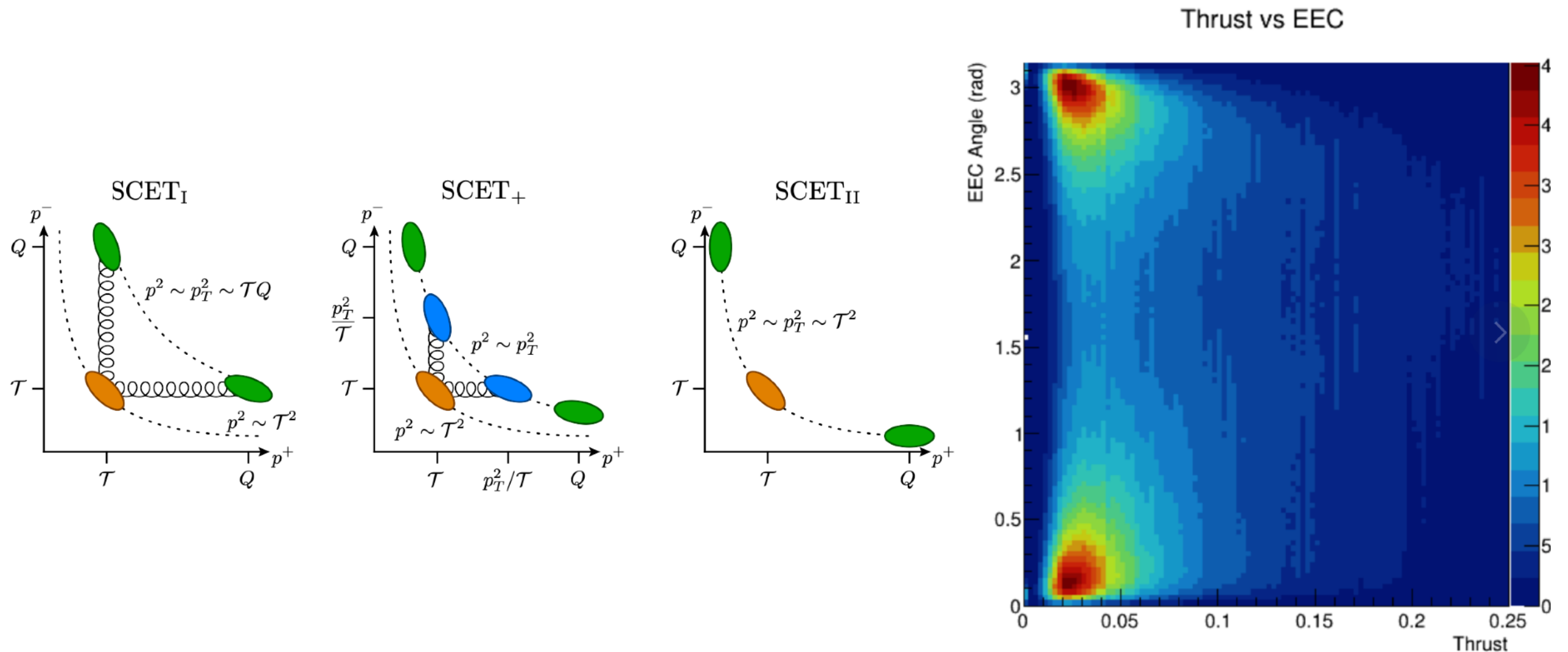
$T \sim 0.5$



$T \sim 1$

EEC at the Belle

- We are working on the joint thrust and EEC resummation in both large and small angle limit Z. Jiang, M. J. Liu & DYS in progress
- Joint TMD and (beam) thrust have been studied in Procura, Waalewijn & Zeune '15; Lustermans, Michel, Tackmann & Waalewijn '19; Makris, Ringer & Waalewijn '21



- The above framework can be generalized to joint thrust and EEC in the large angle limit

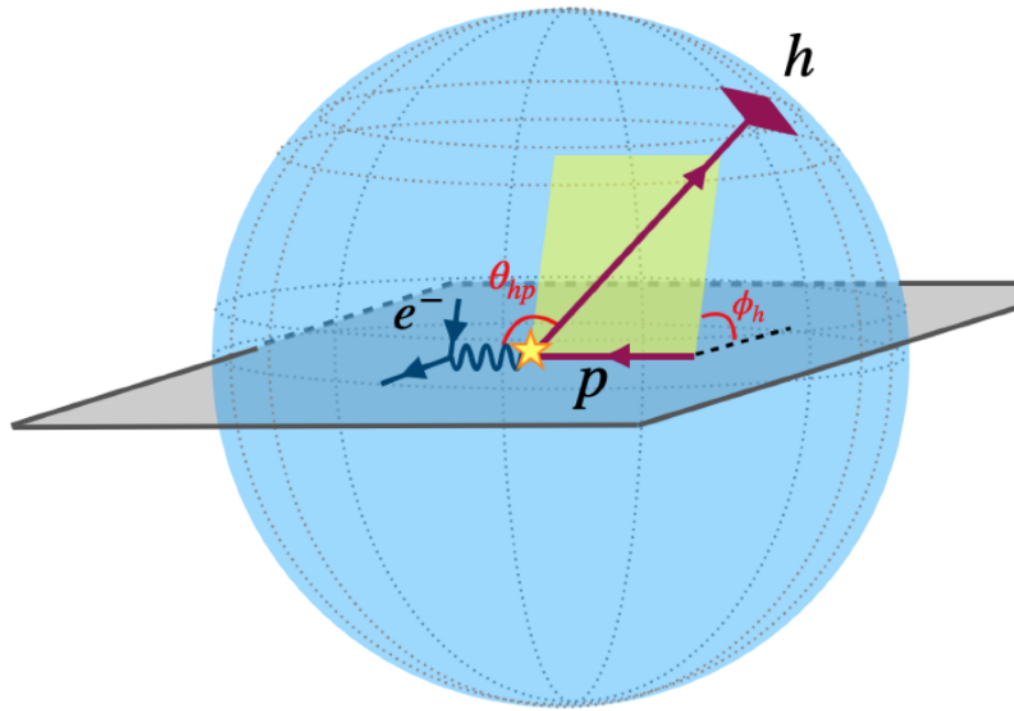
EEC in DIS

The definition of EEC in DIS Li, Marks, Vitev `21

$$\text{EEC}_{\text{DIS}}(\tau) \equiv \frac{1}{2} \sum_a \int d\theta_a dz_a z_a \frac{1}{\sigma} \frac{d\sigma}{d\theta_{ap} d\phi_{ap} dz_a} \delta\left(\tau - \frac{1 + \cos\theta_{ap}}{2}\right)$$

We generalize the above definition

$$\begin{aligned} \frac{d\Sigma_{\text{DIS}}}{dx dy d\tau d\phi} = & \sigma_0 \sum_q e_q^2 \int d^2\mathbf{q}_T \delta(\tau - \frac{\mathbf{q}_T^2}{Q^2}) \delta(\phi - \phi_h) \int \frac{db b}{2\pi} H(Q, \mu) \\ & \times \left\{ J_0(bq_T) \tilde{f}_{1,q} J_q + \cos(2\phi_h) \frac{2(1-y)}{1+(1-y)^2} J_2(bq_T) \frac{b^2}{2} \tilde{h}_{1,q}^{\perp(1)} J_q^\perp \right. \\ & + S_{\parallel} \sin(2\phi_h) \frac{2(1-y)}{1+(1-y)^2} J_2(bq_T) \frac{b^2}{2} \tilde{h}_{1L,q}^{\perp(1)} J_q^\perp \\ & + |\mathbf{S}_{\perp}| \left[-\sin(\phi_h - \phi_s) J_1(bq_T) b \tilde{f}_{1T,q}^{\perp(1)} J_q \right. \\ & + \sin(\phi_h + \phi_s) \frac{2(1-y)}{1+(1-y)^2} \frac{b}{2} J_1(bq_T) \tilde{h}_{1,q} J_q^\perp \\ & + \sin(3\phi_h - \phi_s) \frac{2(1-y)}{1+(1-y)^2} \frac{M^2 b^3}{8} J_3(bq_T) \tilde{h}_{1T,q}^{\perp(2)} J_q^\perp \left. \right] \\ & \left. + \lambda_e \left[S_{\parallel} \frac{y(2-y)}{1+(1-y)^2} J_0(bq_T) \tilde{g}_{1L,q} J_q + |\mathbf{S}_{\perp}| \cos(\phi_h - \phi_s) J_1(bq_T) b \tilde{g}_{1T,q}^{\perp(1)} J_q \right] \right\} \end{aligned}$$



New probe for all TMDPDFs

Collins and Sivers asymmetry of EEC in DIS

Kang, Lee, DYS, Zhao '23 JHEP

$$\mathcal{A}_{\text{DIS}}^{\mathbb{S}} = \frac{2(1-y)}{1+(1-y)^2} \frac{\mathcal{F}_{UT}^{\sin(\phi_{qT} + \phi_s)}}{\mathcal{F}_{UU}}$$

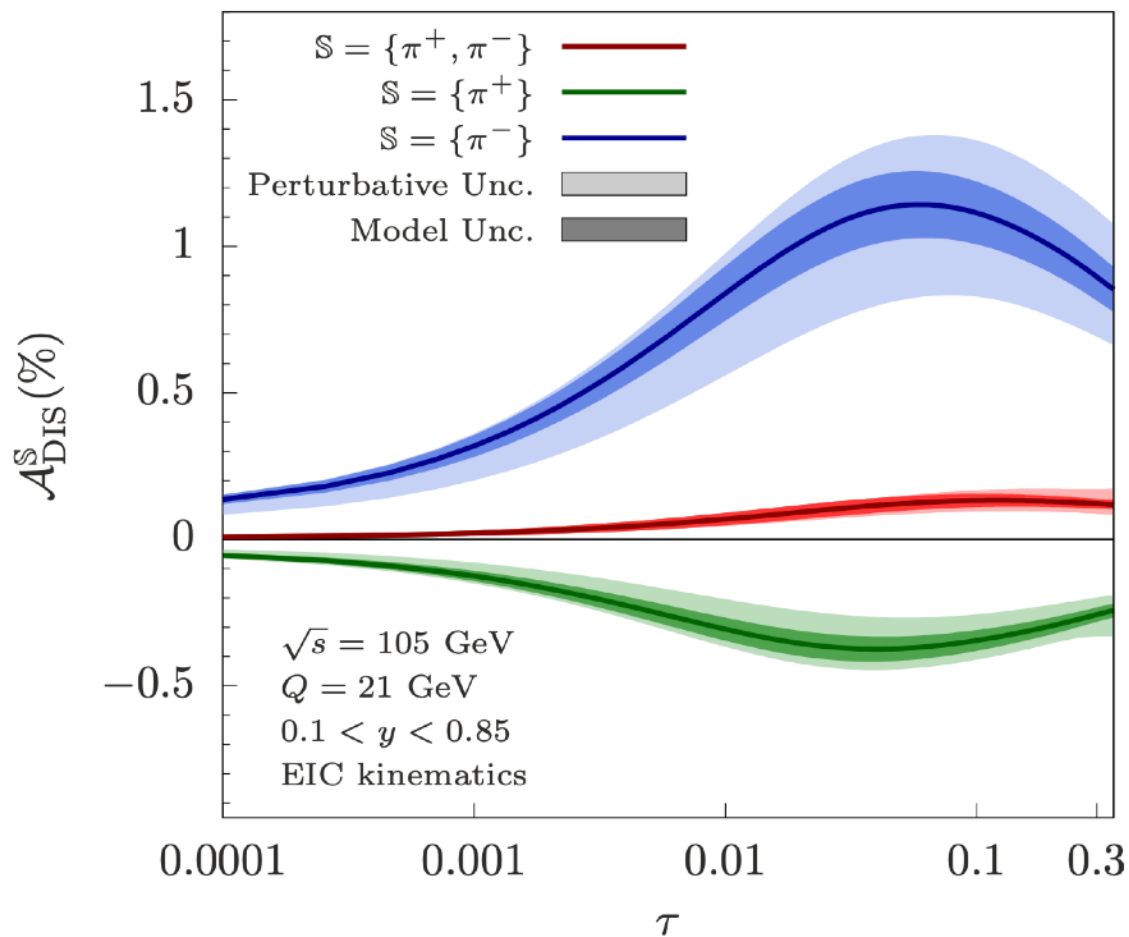
$$\mathcal{F}_{UT}^{\sin(\phi_{qT} + \phi_s)} \sim h_1 \otimes J_q^\perp$$

$$\mathcal{F}_{UU} \sim f_1 \otimes J_q$$

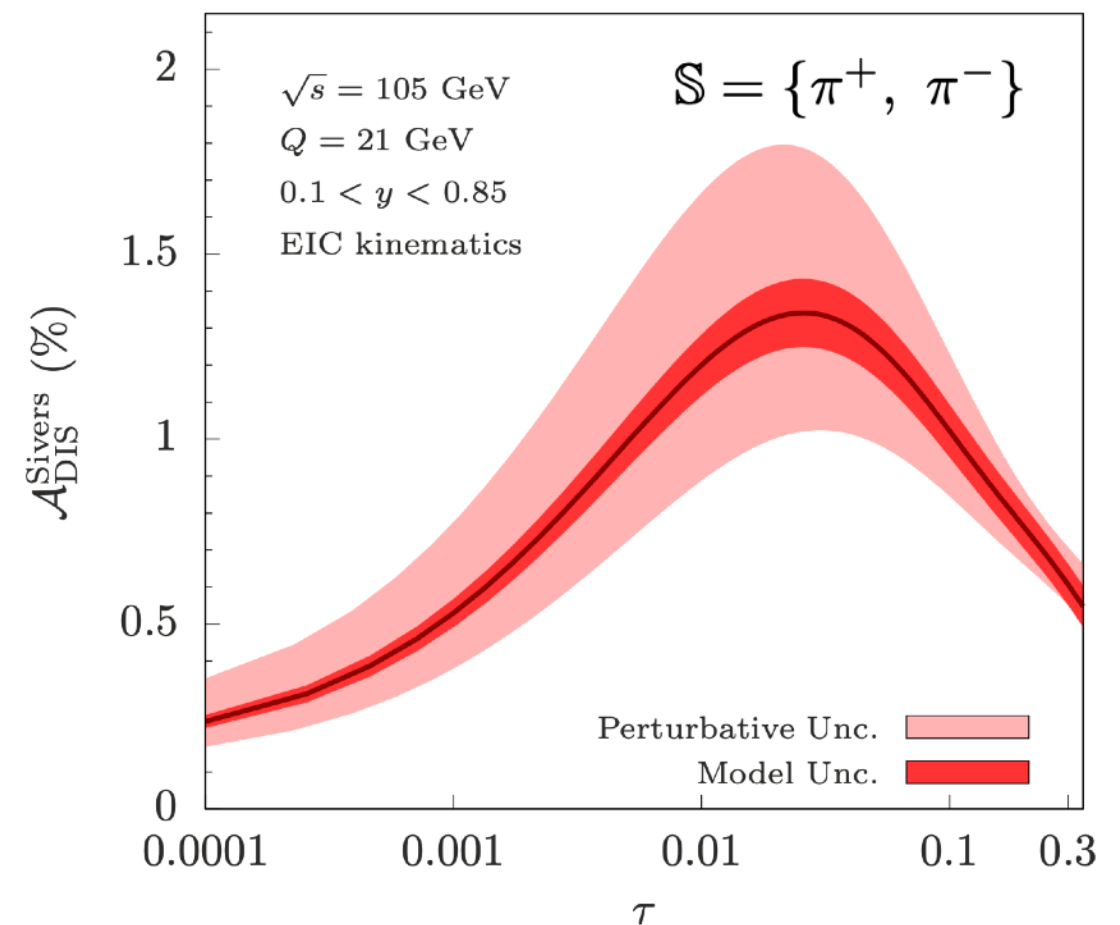
$$\mathcal{A}_{\text{DIS}}^{\text{Sivers}} = \frac{\mathcal{F}_{UT}^{\sin(\phi_{qT} - \phi_s)}}{\mathcal{F}_{UU}}$$

$$\mathcal{F}_{UT}^{\sin(\phi_{qT} - \phi_s)} \sim f_{1T}^\perp \otimes J_q$$

$$\mathcal{F}_{UU} \sim f_1 \otimes J_q$$



Transversity and Collins function
Kang, Prokudin, Sun, Yuan '15



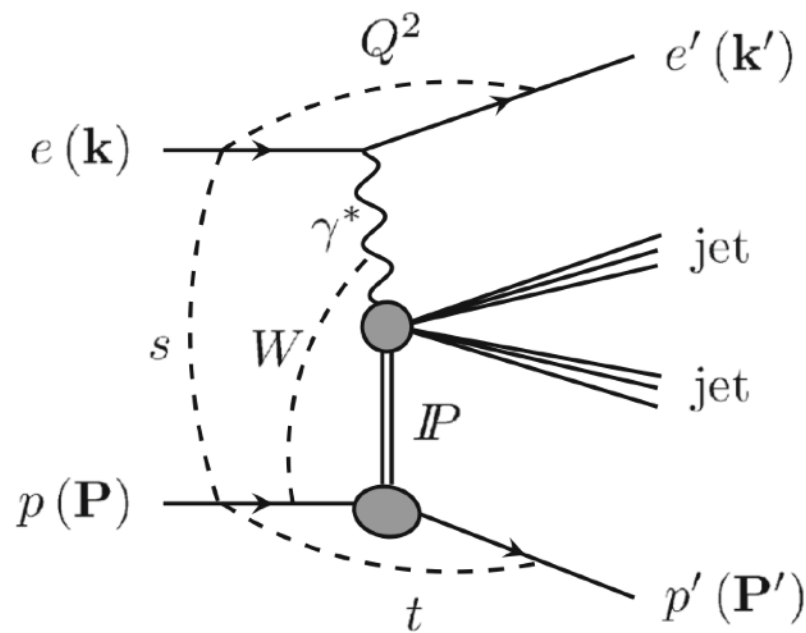
Sivers function:
Echevarria, Kang, Terry '20

Transverse EEC in diffractive dijet production

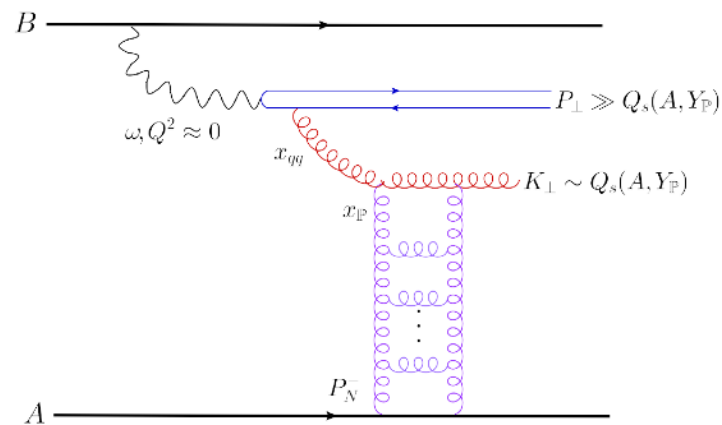
DYS, Y. Shi, C. Zhang, J. Zhou, Y. Zhou '24 JHEP + '24 in progress

Diffractive dijets photo-production

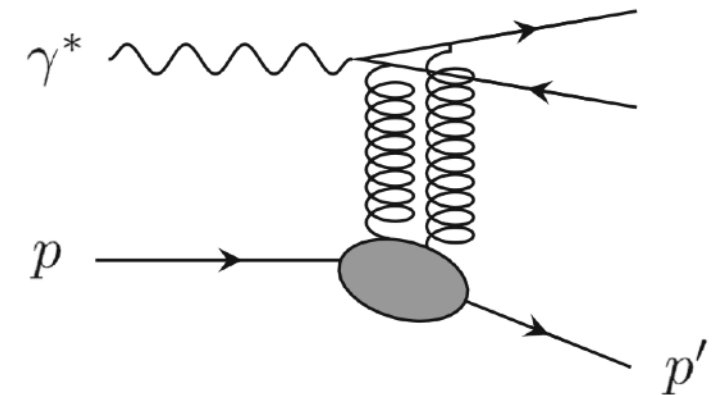
- Diffractive di-jet production provide rich information on nucleon internal structure.



diffractive production of (2+1) jets



diffractive production of exclusive dijets

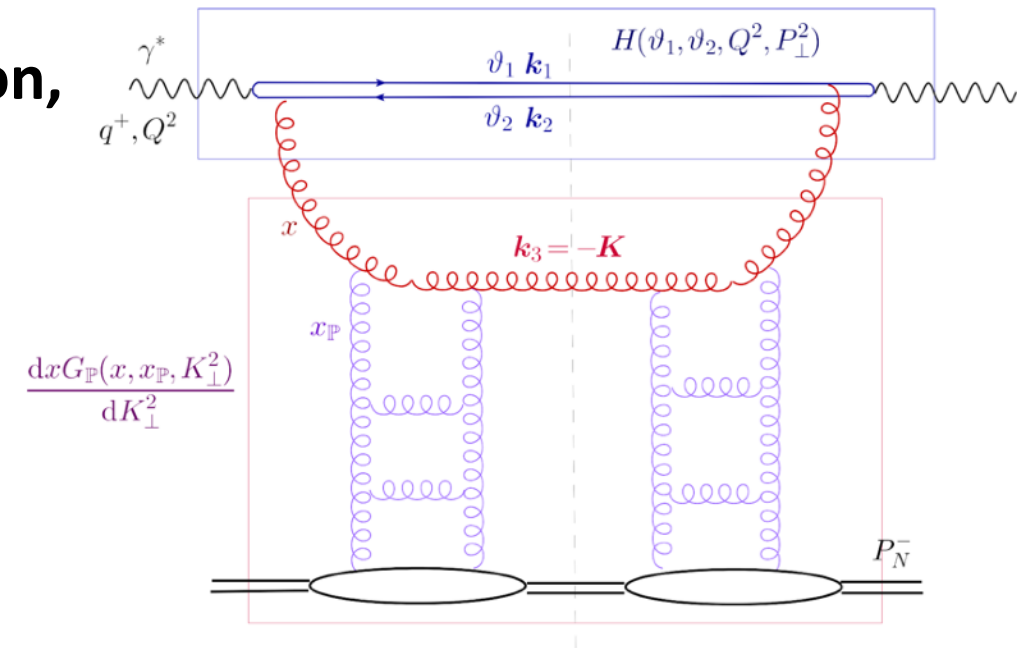


- In cases of diffractive tri-jet production, where a semi-hard gluon is emitted towards the target direction and remains undetected, the experimental signature of this process becomes indistinguishable from that of exclusive di-jet production.
- Recent studies have shown that the cross section for coherent tri-jet photo-production significantly surpasses that of exclusive di-jet production [Iancu, Mueller & Triantafyllopoulos '21](#)
- The production of color octet hard quark-anti-quark dijets enables the emission of soft gluons from the initial state. This mechanism significantly influences the total transverse momentum q_{\perp} distribution of the dijet.

Diffractive dijets photo-production

- The CGC calculation of diffractive di-jet photo-production, accompanied by a semi-hard gluon emission, has been studied in Iancu, Mueller & Triantafyllopoulos '21; Iancu, Mueller, Triantafyllopoulos, & S. Y. Wei '23

$$\gamma(x_\gamma p) + A \rightarrow q(k_1) + \bar{q}(k_2) + g(l) + A$$



- The Born cross section for semi-inclusive diffractive back-to-back dijet production is expressed as

$$\frac{d\sigma}{dy_1 dy_2 d^2\mathbf{P}_\perp d^2\mathbf{q}_\perp} = \sigma_0 x_\gamma f_\gamma(x_\gamma) \int \frac{dx_\mathbb{P}}{x_\mathbb{P}} x_g G_\mathbb{P}(x_g, x_\mathbb{P}, q_\perp)$$

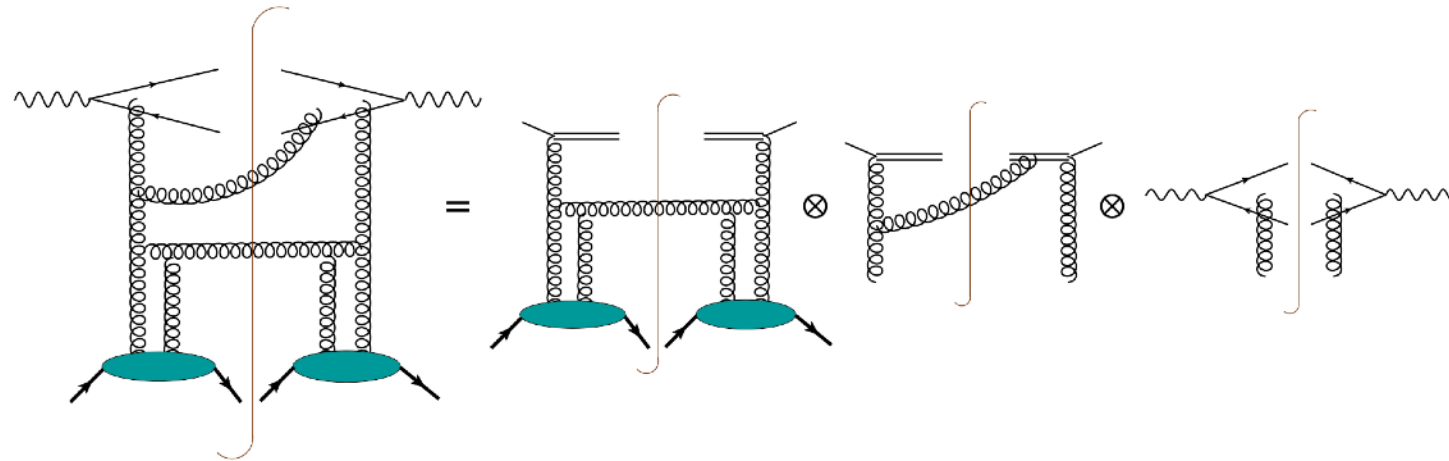
- Within the CGC formalism, the gluon distribution of the pomeron is related to the gluon-gluon dipole scattering amplitude

$$x_g G_\mathbb{P}(x_g, x_\mathbb{P}, q_\perp) = \frac{S_\perp (N_c^2 - 1)}{8\pi^4 (1-x)} \left[\frac{xq_\perp^2}{1-x} \int r_\perp dr_\perp J_2(q_\perp r_\perp) K_2 \left(\sqrt{\frac{xq_\perp^2 r_\perp^2}{1-x}} \mathcal{T}_g(x_\mathbb{P}, r_\perp) \right) \right]^2$$

dipole amplitude

Factorization and resummation

- By treating the gluon DTMD as if it were an ordinary TMD, we assume that the standard TMD factorization framework can be used in the back-to-back region
Hatta, Xiao & Yuan '22



$$\frac{d\sigma}{dy_1 dy_2 d^2\mathbf{P}_\perp d^2\mathbf{q}_\perp} = \sigma_0 x_\gamma f_\gamma(x_\gamma) H_{\gamma^*g}(P_\perp, R, \mu) \int d^2\mathbf{k}_\perp d^2\boldsymbol{\lambda}_\perp \delta^{(2)}(\mathbf{q}_\perp - \mathbf{k}_\perp - \boldsymbol{\lambda}_\perp) \times S(\boldsymbol{\lambda}_\perp, R, \mu) \int \frac{dx_\mathbb{P}}{x_\mathbb{P}} x_g G_\mathbb{P}^{\text{unsub}}(x_g, x_\mathbb{P}, k_\perp, \mu).$$

- We refactorize the gluon DTMD as the matching coefficients and the integrated pomeron gluon function

DGLAP evolution of the pomeron gluon DPDF ?

Glauber SCET Rothstein, Stewart, '16

$$G_\mathbb{P}(x_g, x_\mathbb{P}, k_\perp, \mu, \zeta) = \int_{x_g}^1 \frac{dz}{z} I_{g \leftarrow g}(z, k_\perp, \mu, \zeta) G_\mathbb{P}(x_g/z, x_\mathbb{P}, \mu) + G_\mathbb{P}(x_g, x_\mathbb{P}, k_\perp)$$

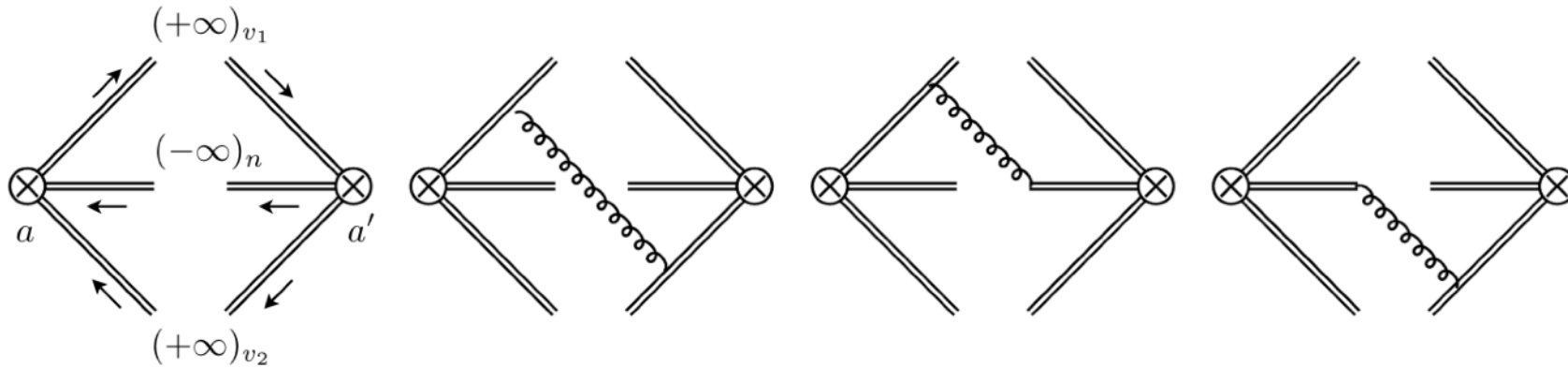
additional static source term in the modified DGLAP equation
Iancu, Mueller, Triantafyllopoulos, & Wei '23

Factorization and resummation

- Resummation formula

$$\frac{d\sigma}{dy_1 dy_2 d^2\mathbf{P}_\perp d^2\mathbf{q}_\perp} = \sigma_0 x_\gamma f_\gamma(x_\gamma) \int \frac{d^2\mathbf{b}_\perp}{(2\pi)^2} e^{i\mathbf{q}_\perp \cdot \mathbf{b}_\perp} e^{-\text{Sud}_{\text{pert}}(b_\perp)} \tilde{S}^{\text{rem}}(\mathbf{b}_\perp, \mu_b) \\ \times \int d^2\mathbf{k}_\perp e^{-i\mathbf{b}_\perp \cdot \mathbf{k}_\perp} \int \frac{dx_{\mathbb{P}}}{x_{\mathbb{P}}} x_g G_{\mathbb{P}}(x_g, x_{\mathbb{P}}, k_\perp),$$

- NLO azimuthal angle-dependent soft function

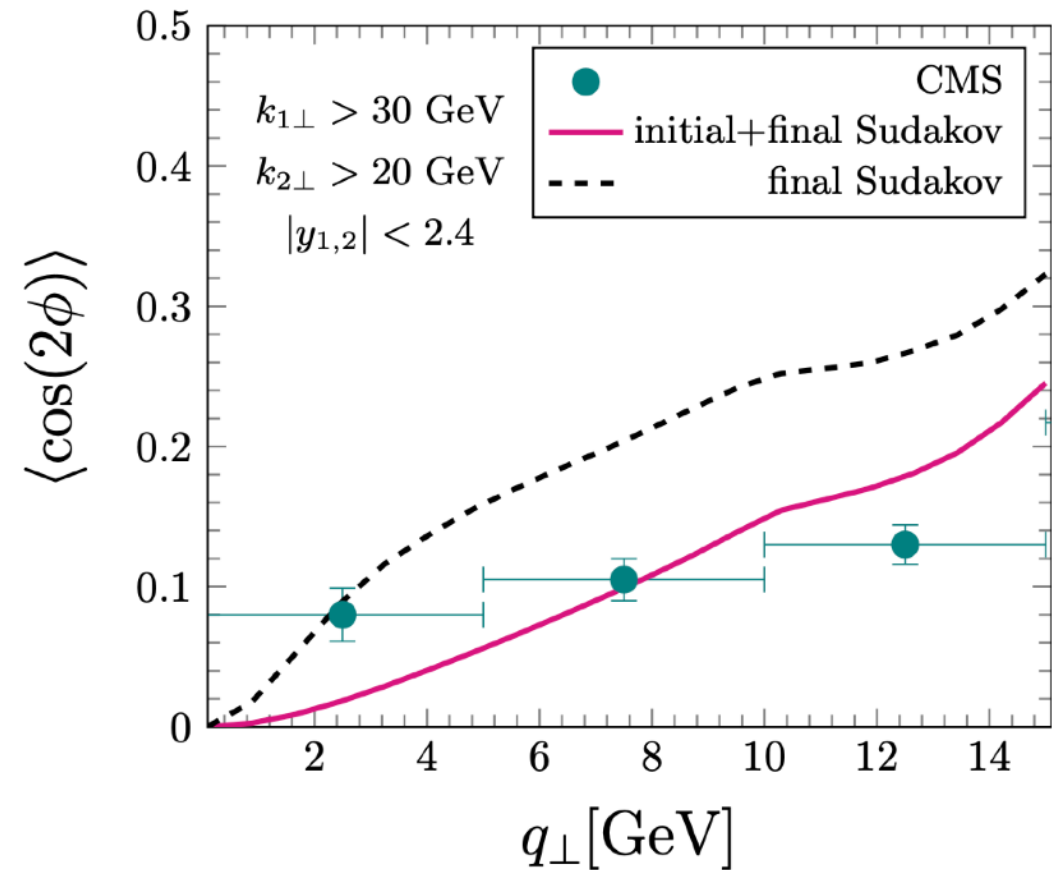
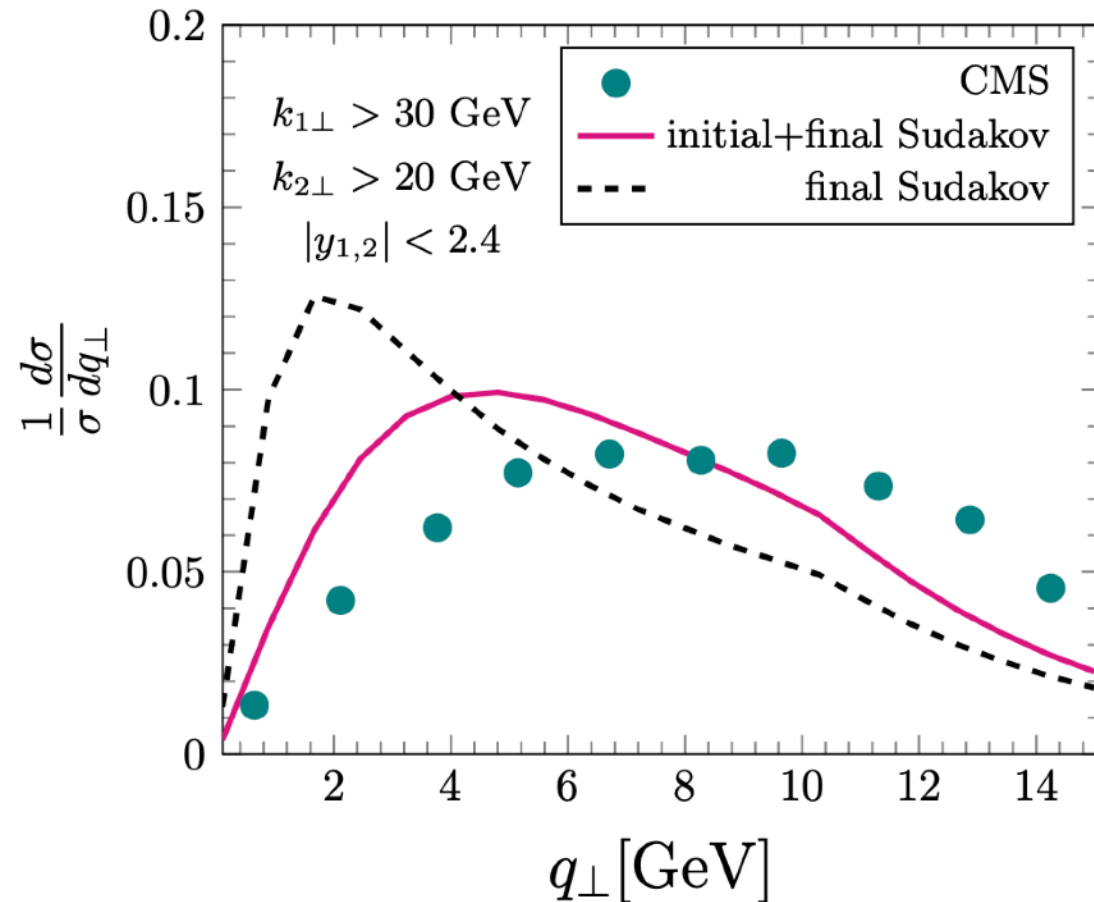


$$\tilde{S}_{\phi_b\text{-dep}}^{\text{NLO}}(\mathbf{b}_\perp, R, \mu_b) = \frac{\alpha_s(\mu_b)}{\pi} \left\{ C_F \left(-\ln \frac{4}{R^2} \ln c_\phi^2 - \frac{1}{2} \ln^2 c_\phi^2 \right) + \frac{1}{2N_c} \left[-\frac{1}{2} \ln^2 c_\phi^2 + \ln c_\phi^2 \ln x \right. \right. \\ \left. \left. - \ln c_\phi^2 \ln \left(1 - \frac{x}{c_\phi^2} \right) + \ln x \log \left(1 - \frac{x}{c_\phi^2} \right) + \text{Li}_2 \left(\frac{x}{c_\phi^2} \right) \right] \right\}$$

$$c_\phi = \cos \phi_b$$

Numerical results and measurements in UPCs

DYS, Y. Shi, C. Zhang, J. Zhou, Y. Zhou '24 JHEP



- Incorporating the initial state gluon radiation offers a more accurate representation of the CMS data
- Difference remains.

$$\langle \cos(2\phi) \rangle \equiv \frac{\int d\mathcal{P} \cdot \mathcal{S} \cdot \cos(2\phi) \frac{d\sigma}{dy_1 dy_2 d^2 P_{\perp} d^2 q_{\perp}}}{\int d\mathcal{P} \cdot \mathcal{S} \cdot \frac{d\sigma}{dy_1 dy_2 d^2 P_{\perp} d^2 q_{\perp}}}$$

The azimuthal asymmetry: Our result underestimates the asymmetry at low q_{\perp} and overshoots it at high

Summary

- We present a comprehensive study of the azimuthal angle dependence of EEC in the back-to-back region to both e^+e^- and ep processes.
- We introduce the Collin-type EEC jet function for the first time.
- By generalizing the EEC with azimuthal angle dependence, one gets access to spin dependent effects (polarized incoming).
- This finding points towards a new approach for gaining a deeper understanding of the complex structure of nucleons.
- We study azimuthal angular asymmetry in diffractive di-jet production. The production of color octet dijets expands the color space, enabling the emission of soft gluons in the initial state.
- This mechanism significantly influences the total transverse momentum distribution.
- Our new results quantitatively capture the overall trends in the q_{\perp} distribution and the asymmetry observed by the CMS Collaboration, a sizable discrepancy between the experimental data and theoretical calculations remains.
- Transverse EEC could provide a complementation study for this mechanism.

Thank you